



Final Report

AGEG Tied Grant 4.1

“Geochemistry, Corrosion and Scaling in Hot Dry Rock Energy Extraction Systems”

16th October 2009

Report Prepared for:

Dr. Tony Hill

Yung Ngothai¹, Brian O’Neil¹, Gideon Kuncoro¹, Allan Pring^{2,3} and Joël Brugger^{2,3}

¹School of Chemical Engineering, University of Adelaide

²School of Earth and Environmental Sciences, University of Adelaide

³South Australian Museum

Executive Summary

An initial study of circulating fluid-rock interactions has been undertaken using a hydrothermal cell which mimics the conditions likely to be encountered at Geodynamics' Habenero site. Key achievements, results and findings from this study are:

1. We have successfully designed and constructed flow-through hydrothermal test rigs which can be used to reasonably accurately mimic the temperature regime of the Habenero geothermal system
2. We have successfully undertaken a series of flow-through experiments in this cell using rock samples from Geodynamics' Habenero site.
3. We observed changes in the mineralogy caused by the changes in fluid composition over a relatively short time frame (a maximum cycle time of three weeks)
4. We have attempted to quantify these changes using a variety of mineralogical and chemical methods.
5. The key finding of this work is that in order to quantify the changes in the rock and fluid composition, you need to spend a considerable amount of time characterizing in great detail the original rock and hydrothermal fluid compositions in the wells. A clear implication of this is that companies should undertake such studies, and also retain and catalog samples.
6. We did not observe any scaling on the pipes over the short time frame of our experiments. Clearly, to study scaling issues longer term (months) experiments need to be undertaken.

1. Introduction

The initial grant (\$100,000) was awarded in 2007 with a starting date of February 1st 2007. The key aims and objectives of this grant are summarised below:

Research Objectives:

Primary objectives were to consider and explore issues relating to hydrothermal geochemistry to ensure safe, economic energy production from “hot rocks”. Key foci were on the following two issues:

- Corrosion and scaling in the pipes: low pH and saline waters at >>200°C are highly corrosive, and it is vital to prevent the generation of scales as the brines are transported to the surface. Specifically, the potential scaling rates due to silica deposition in pipe lines resulting from differences in silica solubility as a function of the changes in temperature difference in the system need to be quantified.
- Maintaining an open pore structure in the reservoir: clogging of the fracture network that allows the brines to exchange heat with the host rock in the reservoir will result in costly shutdowns. Clogging or blockage may occur by precipitation of minerals and/or by hydration of pre-existing minerals with an associated volume increase. Again, these phenomena need to be understood, quantified and ultimately modelled.

To enable achievement of these goals, the project was divided into the following key components & work schedule

Key components:

Involvement of members of the group at the exploration stage to sample the natural groundwater present in the hot rocks; in conjunction with the present-day mineralogy, to ultimately enable calibration of numerical models aimed at predicting the effect of increased fluid flow in situations involving different fluid chemistry scaling.

The Proposed Body of Work:

1. Waters and rocks from the exploration well were sampled to characterise the hydrothermal system and to determine the potential change to mineralogy and pore structure. Clearly the pH of the circulating water is a critical factor as it dictates the likelihood of corrosion rates and heat exchanger fouling. In this preliminary work, we decided to fix the pH for all experiments at 5.5 (the measured pH of the circulating water at the Habenero site).
2. Preliminary experiments were performed to determine the interactions of circulating fluid on rock samples collected from this site. These experiments were performed in the temperature range from 250 to 200°C to mirror conditions at the site.
3. Analysis of data from the above stages enabled our group to identify key issues influencing scaling potential and pore blockage and to identify necessary directions for future work.

2. Background Information

Hot “dry” rock (HDR) geothermal energy has great potential to supply electricity by harnessing stored thermal energy from high temperature granitic rocks in the Cooper Basin and Northern Flinders Ranges. This route provides opportunities for the generation of electrical power without producing greenhouse gas emissions or long-lasting nuclear wastes, at costs competitive with those for energy generated from fossil fuels provided that externalities (e.g. CO₂ taxes) are considered.

Geothermal power is an established energy source in several countries, for example New Zealand and Iceland. However the proposed geothermal operation in South Australia occurs at a much greater depth (5 km) and the heat source is radioactive decay rather than volcanism. In addition, the volume of natural groundwater in these rocks will probably be low, and it is planned to supplement this with surface water from external sources (nearby streams, e.g. Darby’s and Lance’s Bore). Due to the introduction of fresh water to the reservoir, the equilibrium with the surrounding groundwater may be altered.

Currently, literature demonstrates that different HDR reservoirs generate wide variations in the geochemical composition in the circulating water. The key question is “How will the ‘granites’ react when large volumes of water at high pressure move through the rocks?” The granites are currently in equilibrium with surrounding ground water. Their composition is likely to differ significantly from the water pumped through the granite to extract energy. The flow of large volumes of water may cause the partial chemical dissolution or alteration of some of the granites, which could potentially increase the dissolved solids such as silica, and other metals in the circulating fluid. Experiments have shown that the solubility of minerals does not necessarily bear a simple relationship with temperature and pressure; in some cases solubility will decrease with increasing temperature so the metals may dissolve in one part of the granite body and re-precipitate in another section thereby blocking the cracks and fractures. Also the saturation of metals in fluids is volume dependent, very small volumes of fluid require substantial under-cooling before they will precipitate their metals. The complexity of the current system results from the high temperatures (>>200°C) and possibly the high salinity of the fluid (>> 1 wt%). A number of issues relating to geothermal geochemistry are required to be considered and explored to ensure safe, economic energy production from “hot rocks”. Low pH and saline waters at temperatures much greater than 200°C are highly corrosive, and it is vital to prevent the generation of scales as the brines are transported to the surface.

3. Project Phases & Sequencing

It is vitally important to address these issues now, to ensure that the skills and technologies are available locally during production tests. Different HDR reservoirs generate wide variations in the geochemical composition in the circulating water due to differences in the bulk compositions of the host lithologies and the origin of the ground waters. Thus, involvement at the exploration stage will offer the opportunity to sample the natural groundwater present in the hot rocks; in conjunction with the present-day mineralogy, this will enable the calibration of numerical models aimed at predicting the effect of increased fluid flow with a different fluid chemistry and of scaling. The project was performed in three key phases. The initial phase involved a visit to the Geodynamics site at Innamincka to gather samples of the reservoir rock and the circulating water to determine their constituents and composition. The second phase focussed on the design and construction of flow through hydrothermal test cells and preliminary testing of a sample of the collected rock in the hydrothermal cells to demonstrate that it was possible to simulate the conditions likely to be encountered in the fractured reservoir and in the production well (i.e. a temperature gradient from 250 °C to 200°C). Following the success of this phase, a third phase was undertaken involving more rigorous testing in the cell coupled with more advanced mineralogical analysis. A brief summary of key results from each of these phases follows:

3.1: Phase 1: The Habenero Site – Baseline Sampling & Testing

A visit to the Geodynamics site was undertaken by investigators Ngothai, O'Neill Kuncoro. This visit provided us with an understanding of the size and complexity of the site and the consequent processing challenge.

Samples of the reservoir rock and the circulating water were collected. Subsequently, these samples were analysed. Water analysis was performed using solution ICPMS whilst detailed mineralogical studies were undertaken at the SA Museum.

Outlet Fluid Chemistry

This section presents the outlet fluid chemistry obtained from Geodynamics, Habanero 3 Well. The gas analysis and water analysis are presented in Tables 3.1 & 3.2, respectively.

Table 3.1: Headspace gas analysis from Habanero 3 Well

Gas	%v/v
CO ₂ (total)	29.27
Hydrogen Sulfide	n/a
Argon	0.24
Helium	2.93
Hydrogen	0.09
Methane	41.61
Nitrogen	25.85

Table 3.2: Water analysis from Habanero 3 Well (Units mg/L)

Component	1	2	Average
Ammonia (total NH ₃)	0.29	0.27	0.28
Antimony	1.77	1.97	1.87
Arsenic	0.005	0.003	0.004
Barium	13.6	18.4	16
Boron	223	222	222.5
Calcium	26.6	24.3	25.5
Calcium hardness	66	61	63.5
Chloride	8110	8360	8235
Fluoride	17	17	17
Lithium	246	251	248.5
Magnesium	0.5	0.4	0.45
Potassium	637	650	643.5
Rubidium			
Silica (as SiO ₂)	150	156	153
Sodium	3790	3830	3810
Sulfate	37.2	34.8	36
Uranium	< 0.005	< 0.005	0.005
H ₂ O			94640.
CO ₂ (total), mg/L	549.5		549.5
Argon	4.099		4.099

Helium	5.34		5.34
Hydrogen	0.080		0.080
Methane	283.3		283.3
Nitrogen	329.5		329.5

Rock Analysis

Petrographic analysis was undertaken of rock chip samples from Habanero 3. A photomicrograph of the rock sample from Habanero 3 in thin section is shown in Figure 3.1. The rock is composed of feldspar syenite, with albite (A), and microcline (K) with carbonate alteration. This indicates that the rock has been subjected to hydrothermal alternations.

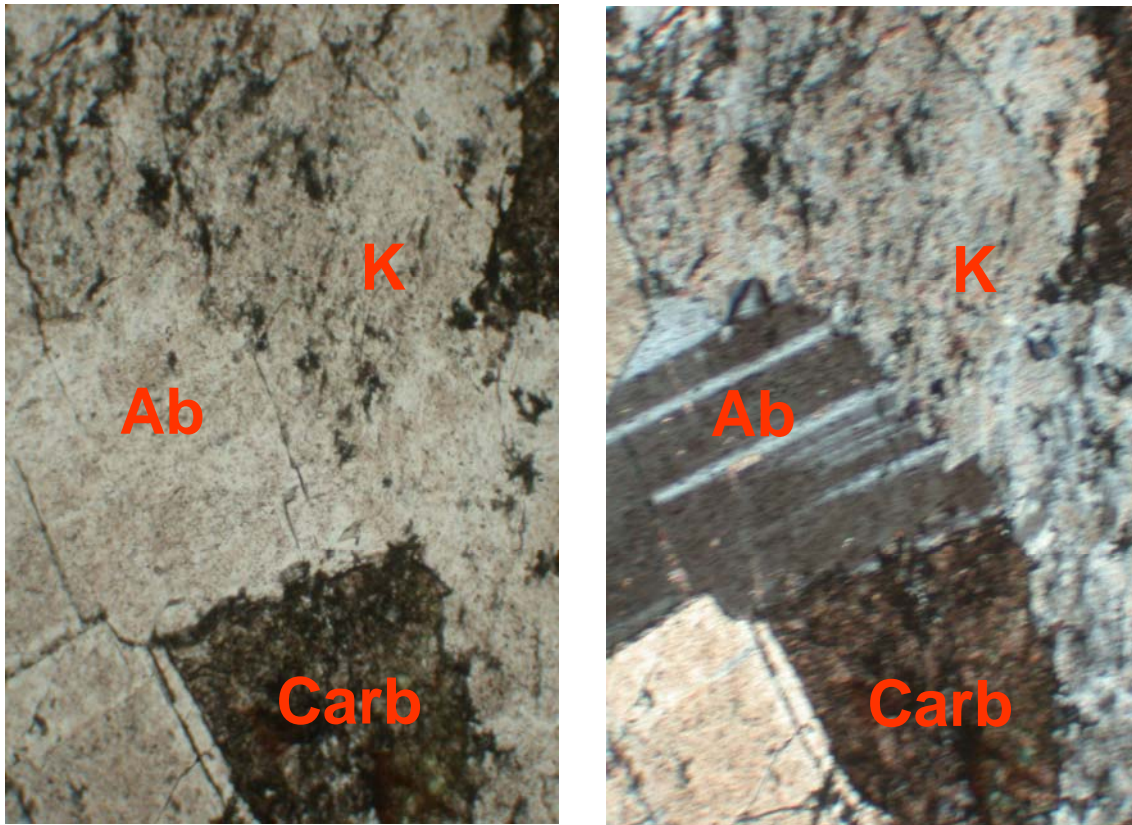


Figure 3.1: Host rock Habanero 3: “syenite” consisting of albite (Ab), microcline (K) with extensive carbonate (Carb) alteration – field of view 2 mm across

The rock sample from Habanero 3 appears to be a feldspar syenite composed chiefly of albite, near end member composition and microcline which has a mottled texture with relatively little quartz.

3.2 - Phase 2: Initial Hydrothermal Testing

This phase involved the design and construction of a flow-through hydrothermal cell in which we have created an environment similar to that encountered in the reservoir and the outlet well. These initial studies confirmed that the required environment could be provided by such a cell.

Hydrothermal Flow-through Cell

In order to investigate the fluid-rock interaction, a hydrothermal flow through cell has been developed. A diagram and a photograph of the flow through cell are provided in Figure 3.2.

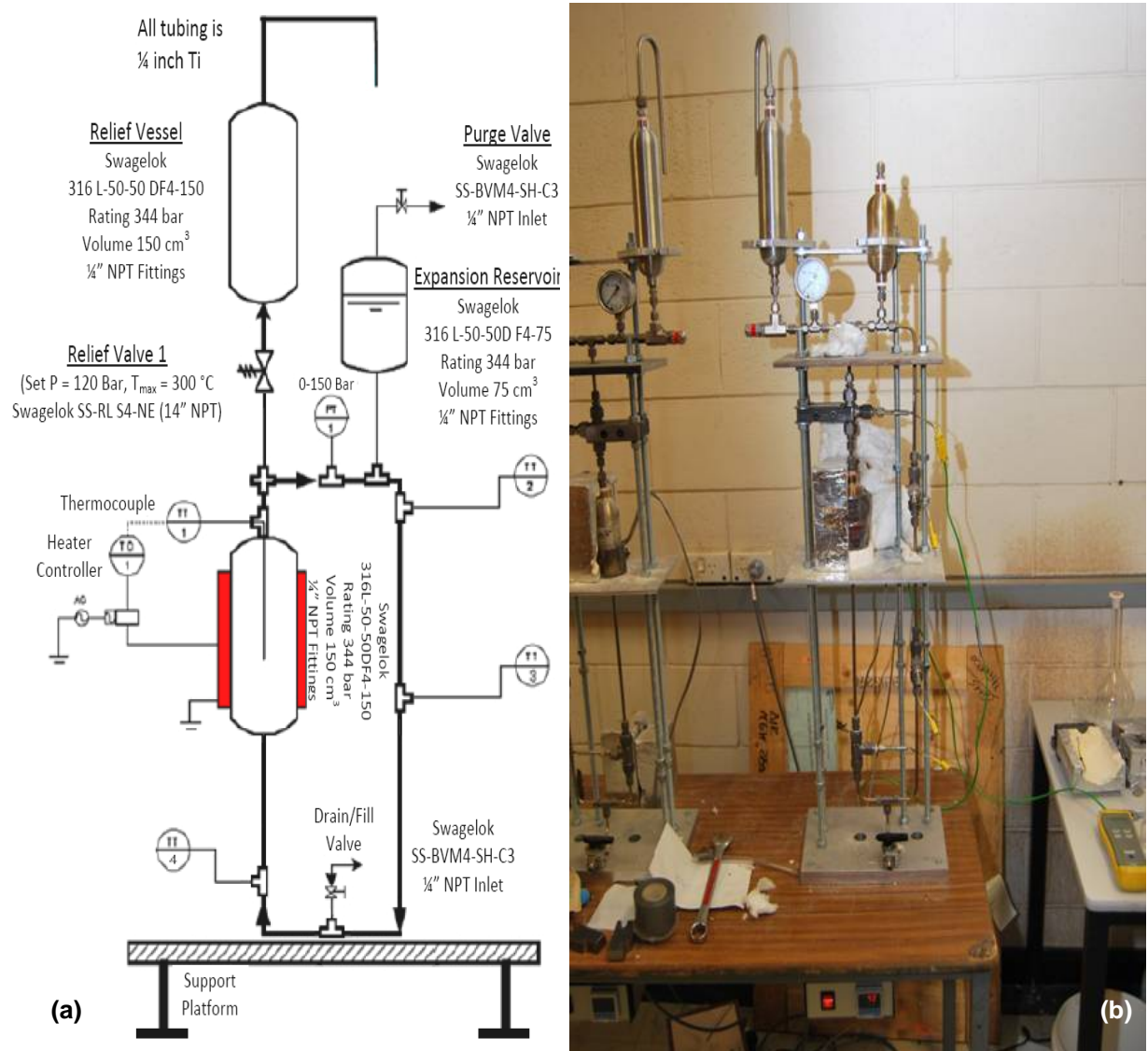


Figure 3.2 Hydrothermal flow through cell (a – schematic & b – photograph)

The cell is designed to operate in a flow-through configuration where the fluid circulates continuously inside the cell. The driving force is provided by the thermosiphon effect (the hot side being less dense rises whilst the denser cold side falls). The total cell volume is 345 mL. All tubing is constructed from ¼ inch SS and connected with standard Swagelok SS fittings, with the reservoirs in stainless steel (SS316). The total length of the cell loop is approximately 1800 mm. The volume of the main reservoir is 150 mL. A pressure relief vessel is employed to the cell for safety. The volume of the relief vessel is 300 mL and the relief valve was set to open at a maximum pressure of 100 bar. An expansion reservoir is employed to compensate for changes in volume as the fluid is heated. The volume of the expansion reservoir is 150 mL. All vessels are rated at 344 bar. Four thermocouples are installed to monitor the temperature changes throughout the cell. A pressure transducer is installed to monitor the pressure. The operating temperature and pressure are 250°C and 40 - 50 bar, respectively. Temperature is controlled by a simple relay controller and two heaters are used and arranged in parallel. The ring type heaters are bolted to the main reservoir and insulated with ceramic bricks.

Flow-through Cell Results

This section presents the preliminary analyses of the rock-water interaction using the hydrothermal cell. The temperature profile, XRD result of the rock sample, and ICP-MS analysis on the circulating water are presented and discussed in this section. The hydrothermal test was conducted for a constant 4 day cycle.

Preliminary Temperature Profile

The temperature profile of the hydrothermal cell is given in Figure 3.3

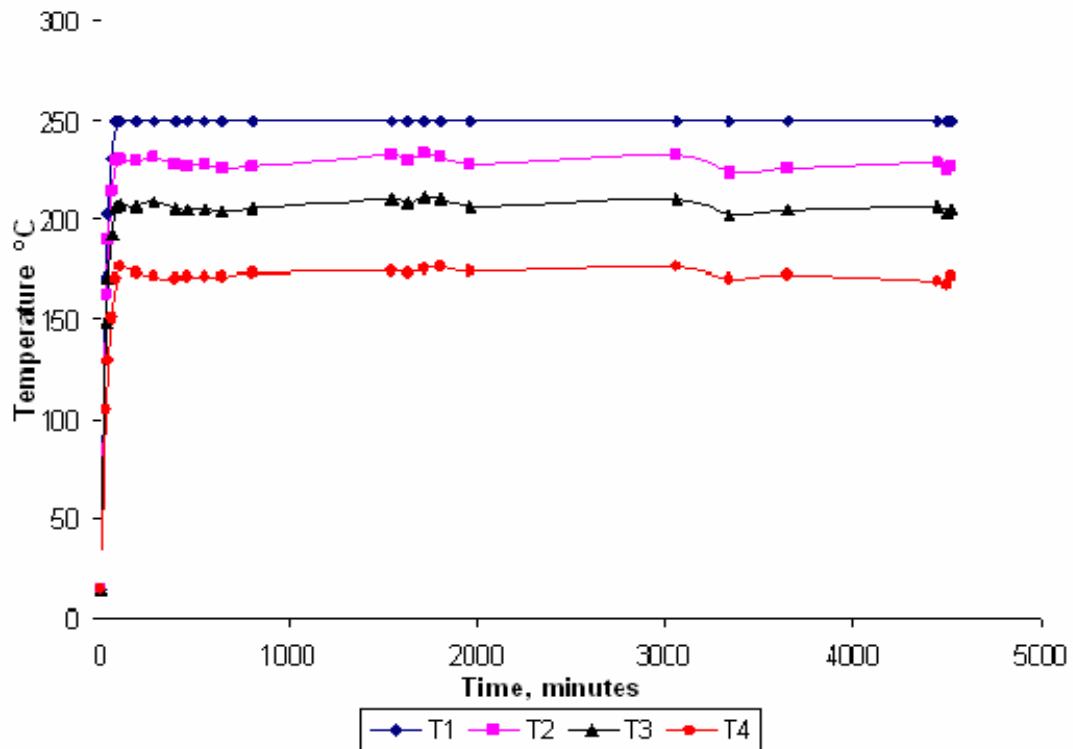


Figure 3.3: Temperature profile of fluid-rock interaction experiment

The above results showed that the temperature variations are minimum and stable. The set point of 250°C has been achieved and assumed to represent the condition of the actual rock-water interaction in the bore hole. Since the circulation of water in the hydrothermal cell is promoted by density change as a function of temperature, the temperature difference (ΔT) obtained were adequate. The pressure inside the cell is approximately 40 – 50 bars and remained constant over the experimental period (4 days).

Preliminary Rock Analysis

XRD analysis on the rock sample from geothermal cell experiment is presented in

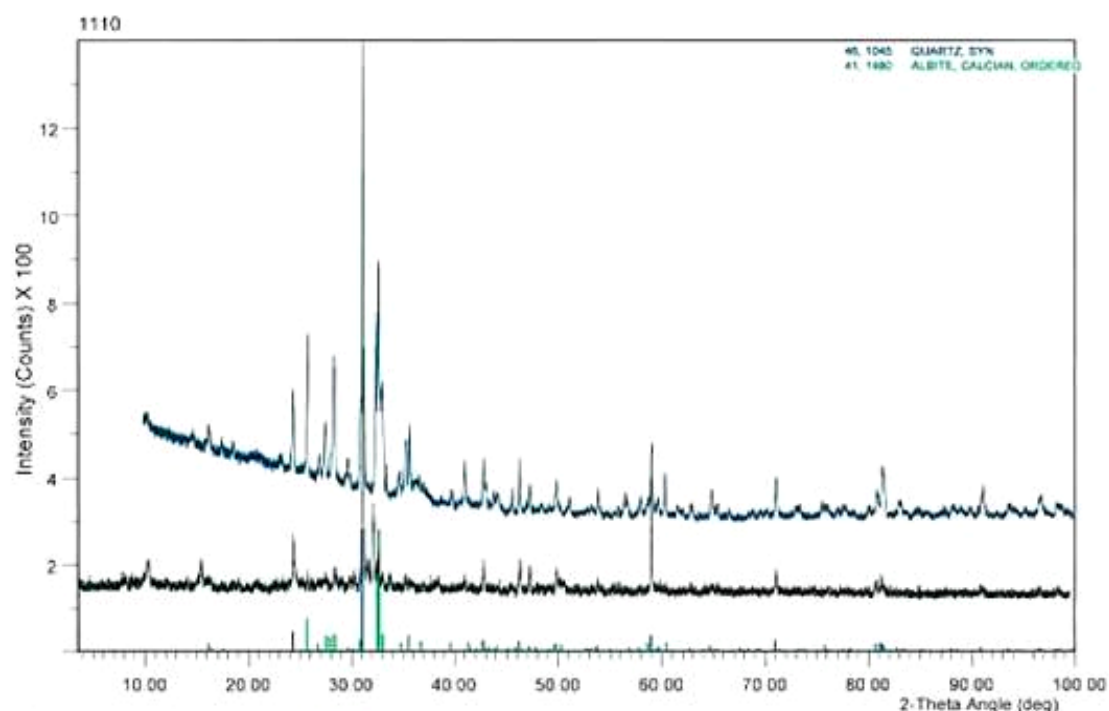


Figure 3.4 X-ray diffraction pattern of starting rock sample compared with rock sample after 4 days in cell.

Figure 3.4 shows that nearly all the albite feldspar has dissolved. However, the circulating fluid used was distilled water and with a fine rock grain sample size (100 – 200 μm) was used for the experiment. This preliminary result suggests that with pure water and fine grain size, the interaction between the rock and circulating fluid occurs rapidly.

Water Analysis

Figure 3.5 presents the results of the ICP-MS analysis on the circulating water after four, seven and fourteen days of rock-water interaction. The results for 7 and 14 days (further work) are included to see the influence of circulation period. Clearly, the concentration of most of the element decreases with time. This indicates that precipitation has occurred. Analysis of SiO_2 was not performed as ICP-MS has silica interference. In later trials, silica will be analysed using Hach methods.

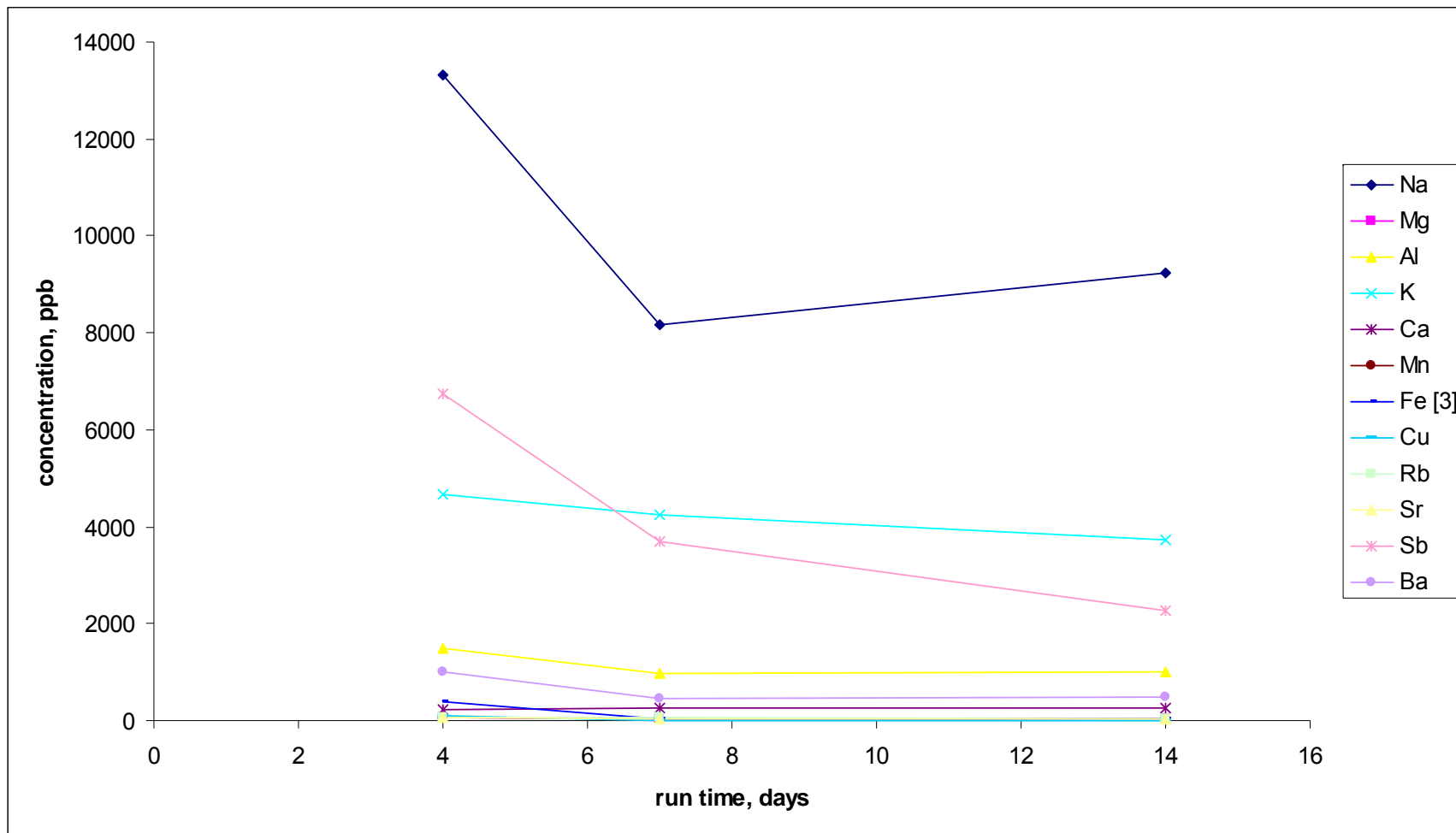


Figure 3.5 ICP-MS analysis of the circulating water as a function of time of contact

3.3 Phase 3: Further Work

Following the completion of Phase 2 and the successful demonstration of the thermosiphon cell as an appropriate tool a more detailed study of the system was commenced. As with the previous phase, water analyses were performed using ICPMS, whilst silica was quantified with the Hach spectrophotometer. Detailed mineralogical analyses of the rock samples were performed by the SA Museum using XRD (X-ray diffraction), XRF (X-ray fluorescence) and SEM (Scanning Electron Microscopy). A summary of the results and key findings follows.

Concurrent with these analytic studies, a series of new and improved cells were designed and constructed in Titanium. This choice will allow us to test highly corrosive circulating fluids (e.g. high salinity – up to 1% sodium chloride) As well, cells with larger sample chambers have been constructed. These cells are currently undergoing testing to refine and optimize their design.

Results & Discussion

This section summarises the results of detailed analyses on the rock and fluid samples obtained from the hot dry rock geothermal site in Cooper Basin. Results of rock-water interaction experiments are also presented here, including the analyses of rock and water.

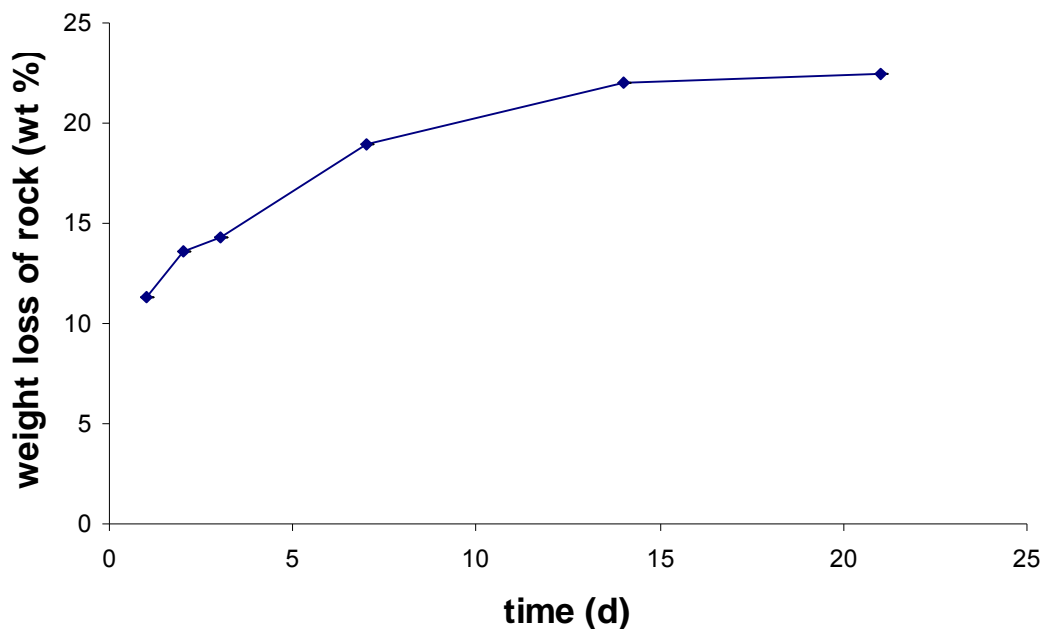


Figure 3.6: Weight loss of the rock (% w/w) versus time

Figure 3.6 shows the mass of rock dissolved to solution. Clearly, the mass of rock dissolved to the solution increases with time. The dissolution rate appears to be more rapid in the early stages of the experiment due to the dissolution of finer particles present in the rock sample.

In order to confirm the dissolution rate with eliminate the effects of the fine particulates, rock samples were ultrasonically cleaned. The cleaning of an initial rock sample weighing 5.11 g resulted in the loss of only 0.021 g of the sample. Hence, approximately 0.41 wt% of the sample dissolved. Further experiments are needed to accurately quantify the changes in dissolution rate using the cleaned samples.

A second set of experiments was performed to observe the effects on dissolution when circulating newly injected fresh water. This set of experiments was intended to accelerate the dissolution reaction and to replicate the condition in the actual geothermal plant if the dissolved minerals were precipitated in a precipitation tank, whereupon a less saturated liquid would be reinjected to the bore hole.

Experiments at circulation times of 17hours, 7 days and 14 days were conducted with water replacement every 24 hours. An empty sample basket was also positioned in the T_4 temperature point (the lowest temperature in the loop) in order to observe any deposition that may have occurred during the experiment run. The first experiment (e.g. 17 hours) was originally planned to run for 24 hours.

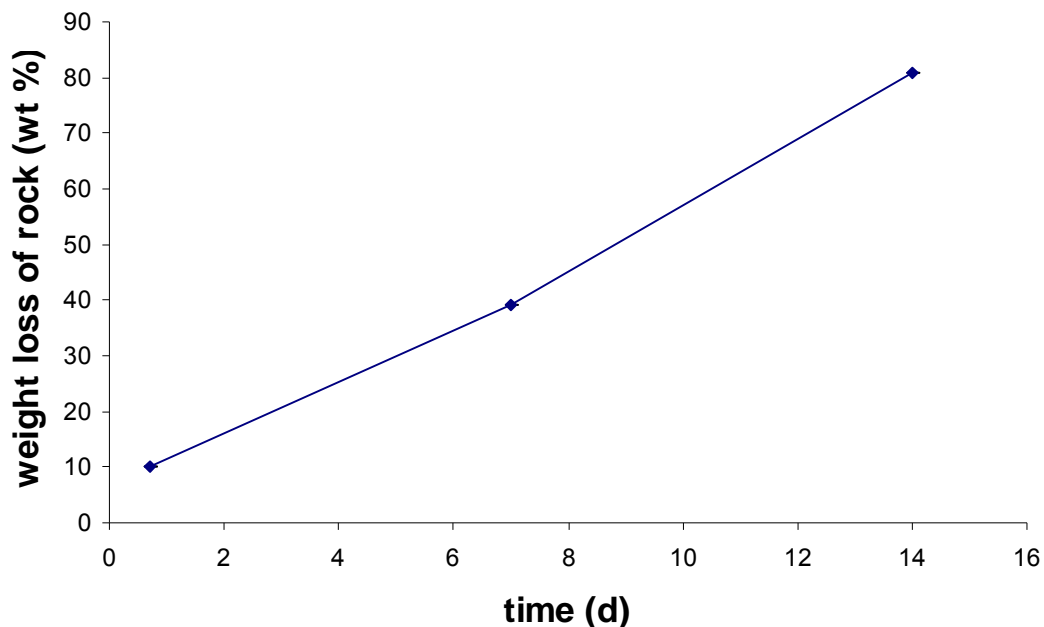


Figure 3.7: Rock weight loss (% w/w) versus circulation time with ultrasonically cleaned samples coupled with fluid replacement every 24 hours

Figure 3.7 presents the dissolution results for this sequence of tests. The clear consequence of fluid replacement is a significant increase in the rate of dissolution (as expected).

The following Figures 3.8 – 3.12 present a temporal sequence of SEM images of the rock sample surface. These images were obtained using the secondary electron detector from Philips XL30 located at Adelaide Microscopy Centre. The SEM images provide clear evidence of the presence of fine particles adhering to the surface of the rocks. These fine particles disappear (dissolving into the circulating liquor) as the experiment proceeds. Simultaneously, the roughness of the surface of the rocks becomes more apparent. Etch pits are then evident on the surface of the rocks and continue to develop in the later stages of the experiment. Clearly, weathering and dissolution of the rock increase with interaction time.

SEM Images of the Rock Samples

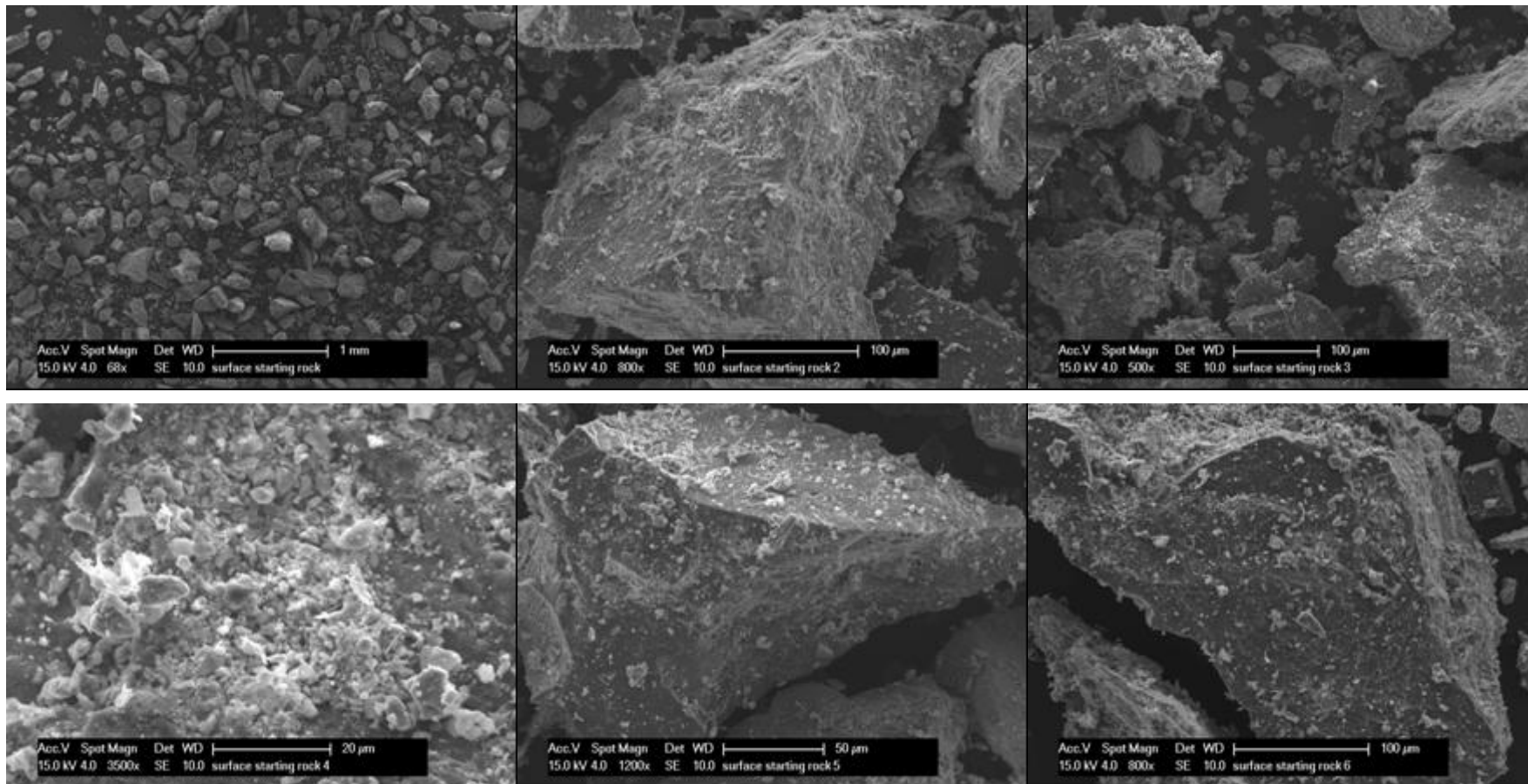


Figure 3.8: SEM images of the initial rock samples

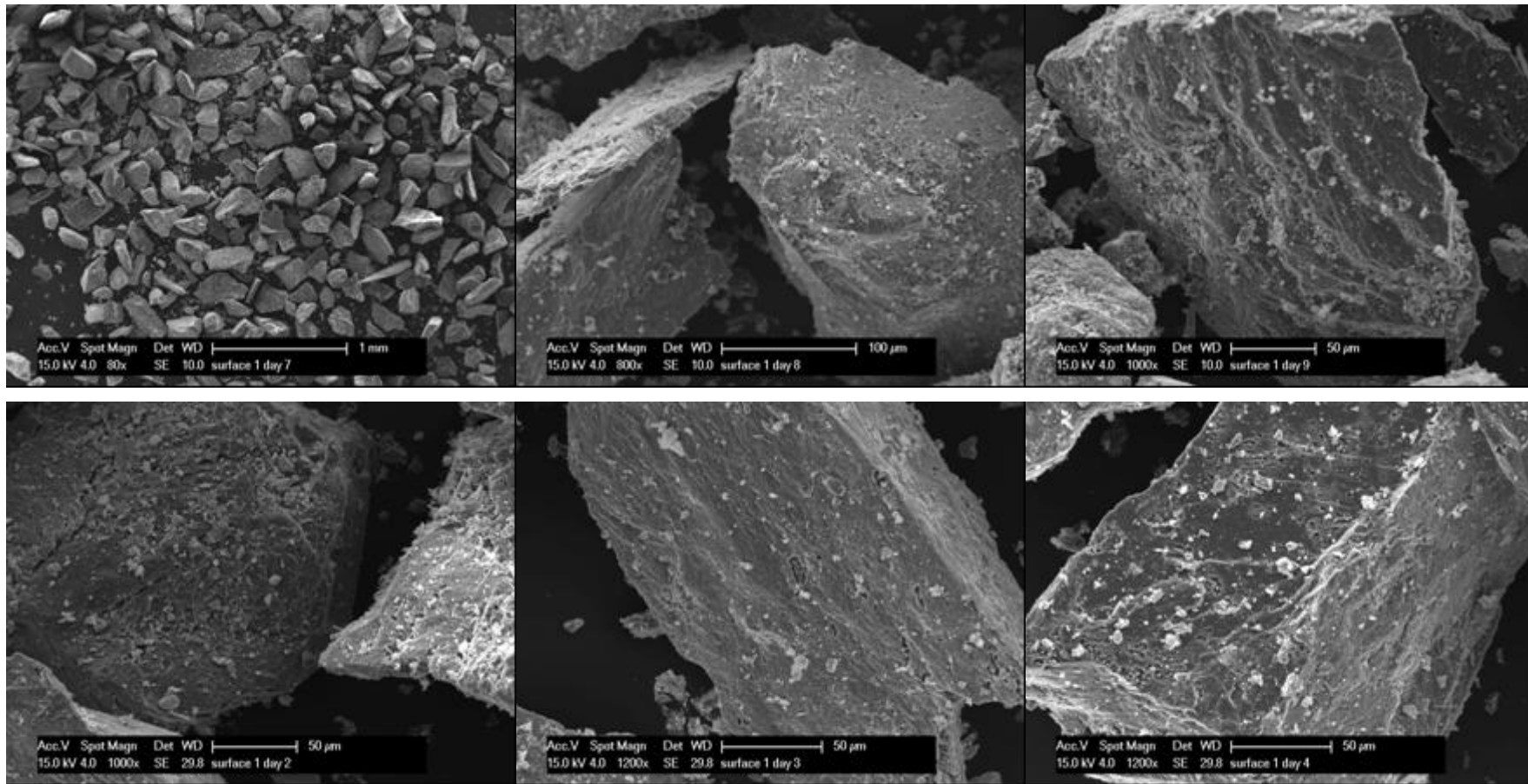


Figure 3.9: SEM images of the rock samples after 1 day

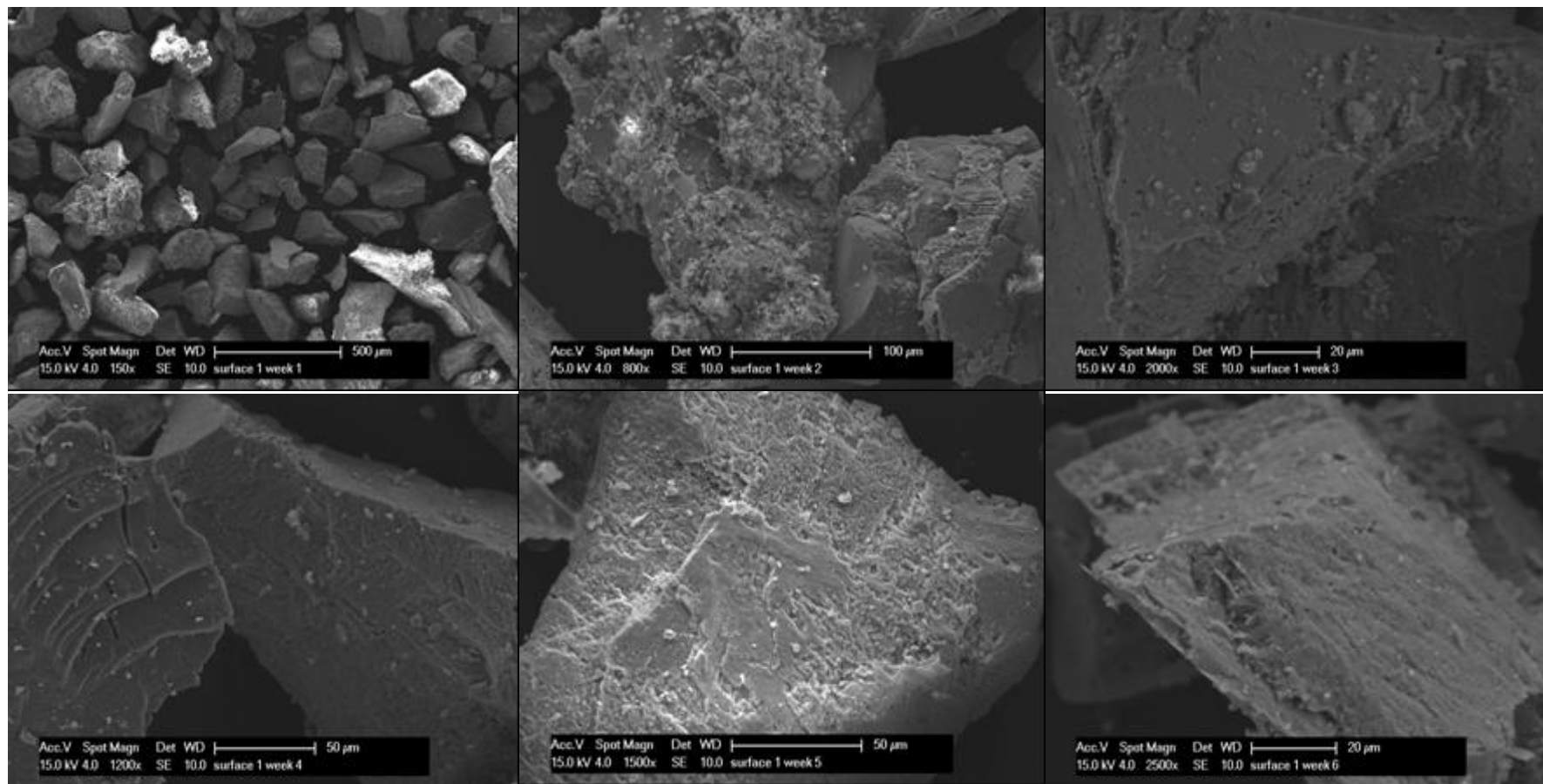


Figure 3.10: SEM images of the rock samples after 7 days

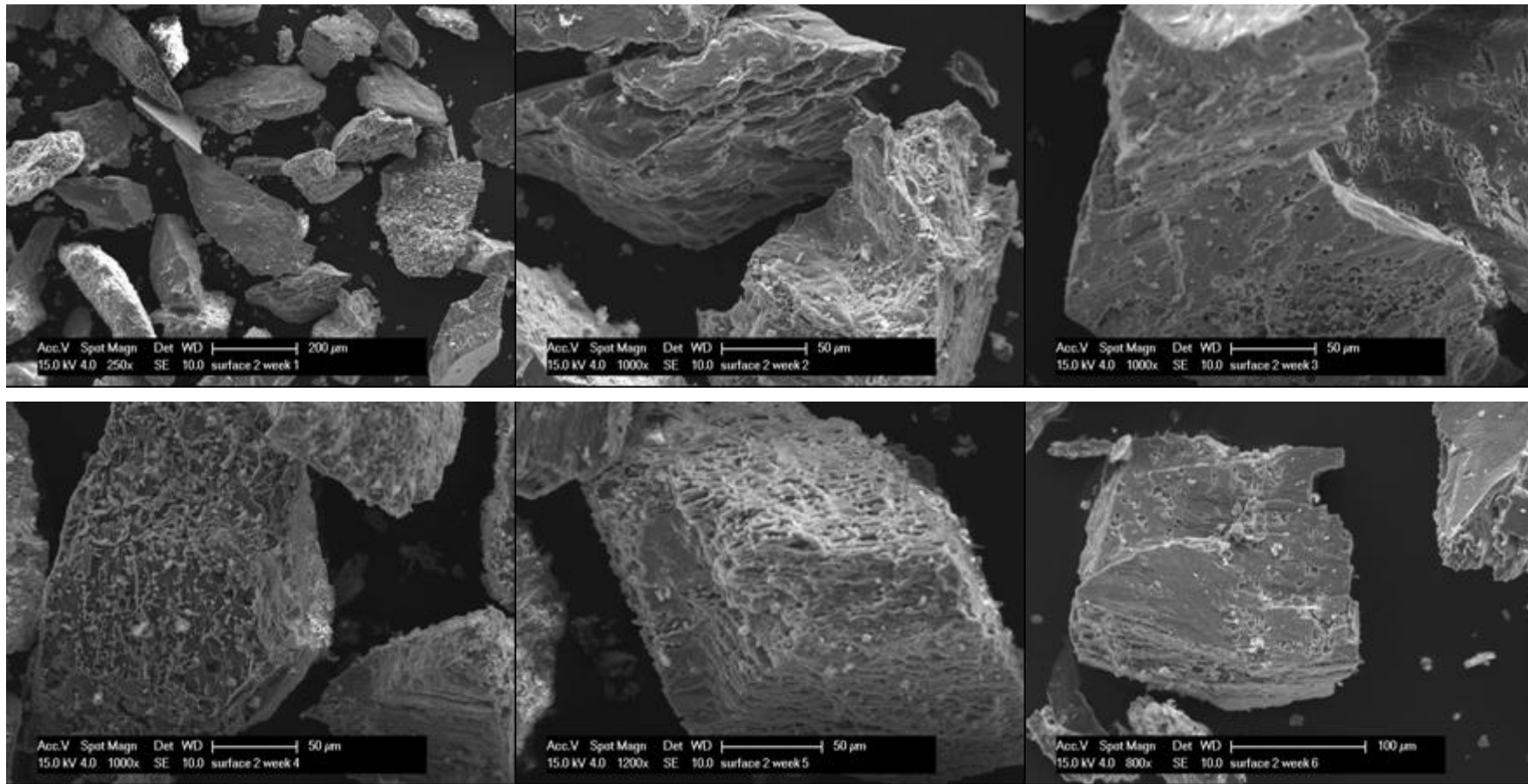


Figure 3.11: SEM images of the rock samples after 14 days

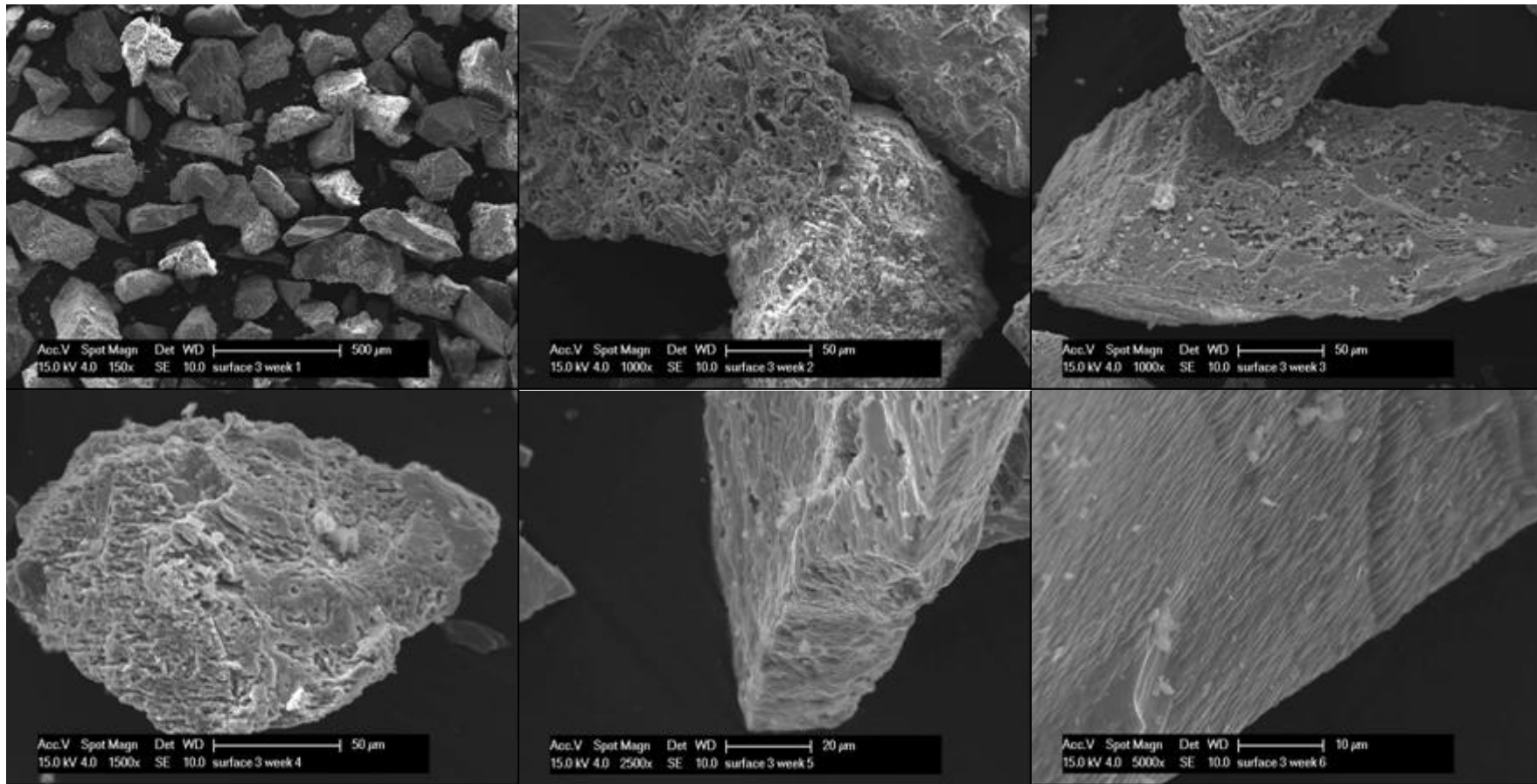


Figure 3.12: SEM images of the rock samples after 21 days

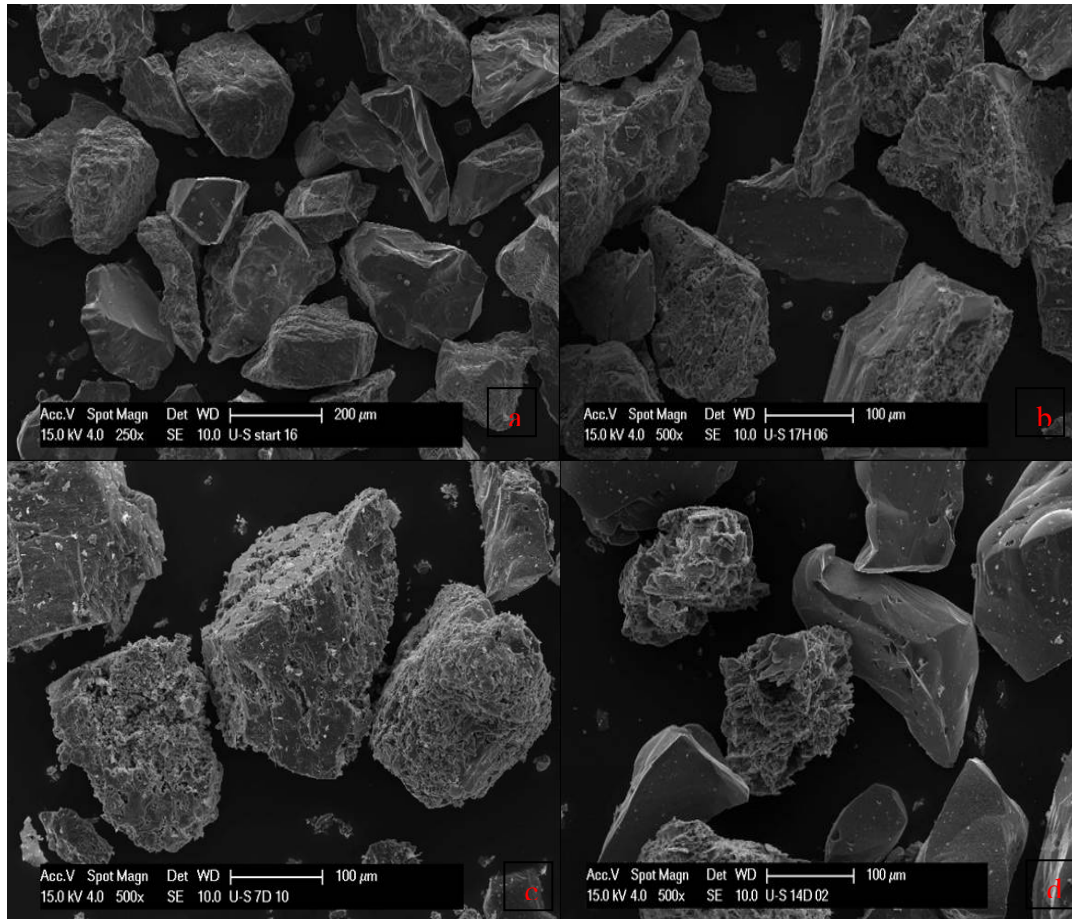


Figure 3.13: SEM images of the rock samples: (a) initial sample, (b) after 17 hours (c) after 7 days and finally (d) after 14 days. In the final image, most of the feldspar has been dissolved leaving mainly smooth quartz grains

Figure 3.13 presents a temporal sequence of SEM images of the sample rock surfaces for ultrasonically cleaned samples with circulating fluid replacement every 24 hours.

The images confirm that fine particles are absent in the initial rock sample following ultrasonic cleaning. The images also show increasing roughness of the rocks as the reaction proceeds. More severe etch pitches are observed at longer experimental times, clearly indicating increased mineral dissolution to the circulating water with fluid replacement every 24 hours.

Furthermore, fine particles are observed after 7 days' circulation (Figure 3.13-c). These are probably a consequence of the dissolution reaction, where the rock samples (e.g. feldspars) break down to smaller and finer particles. The fine particles

are no longer present in the 14 day images (Figure 3.13-d). Clearly, these particles have dissolved to the liquid phase. The backscattered image following 14 days of circulation suggest that the samples are becoming more homogenous with quartz as the dominant remaining mineral.

Backscattered SEM Images of the Rock Samples

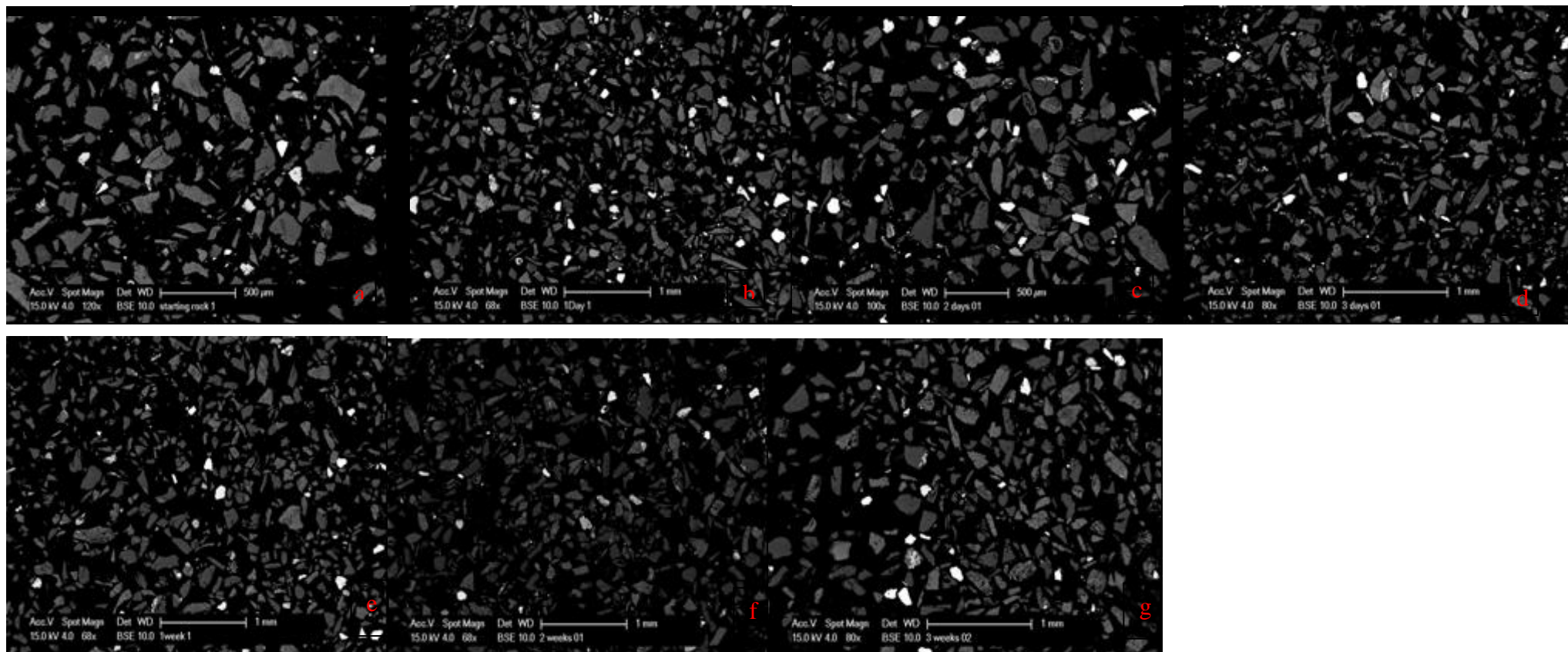


Figure 3.14: Backscattered images of the rock sample: (a) initial sample at time = zero, (b) 1 day later, (c) 2 days later, (d) 3 days later, (e) 7 days later, (f) 14 days later, and finally (g) after 21 days

Figure 3.14 presents backscattered SEM images of the rock samples at various sampling times. These images were produced by using the backscatter electron detector from XL30 at the Adelaide Microscopy Centre. Clearly, there are several mineral phases present in the samples. Using the spot scan option, the minerals can be semi-quantified and identified.

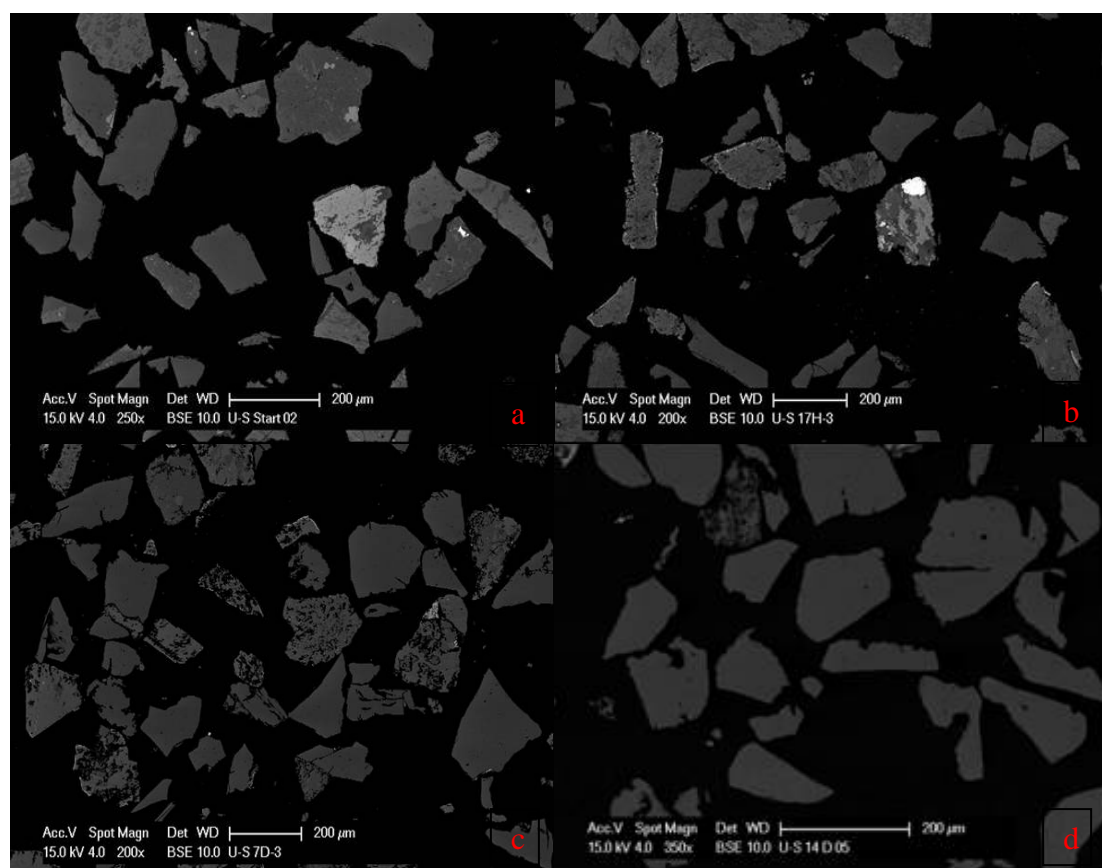


Figure 3.15: Backscattered SEM images of the rock sample: (a) initial sample, (b) 17 hours later, (c) 7 days later, and finally (d) after 14 days.

Figure 3.15 provides backscattered images of ultrasonically cleaned samples (again with fresh circulating fluid added every 24 hours). Again, the dominant mineral phase is quartz but traces of accessory minerals still remain.

Mineral identification studies identified quartz, feldspar (albite), and microcline as the major species. The feldspar was variably veined and included patches of fine grained carbonate with a magnesium and iron-rich composition. The rock also contains minor amounts of pyrite (FeS_2), sphalerite (ZnS), fluorapatite ($\text{Ca}_5(\text{PO}_4)_3\text{F}$). There are also some traces of fluorite (CaF_2), barite, and a titanium oxide mineral

(probably rutile or anatase). Preliminary observations suggest little alteration of the major mineral phases. However, it is clear that the carbonates dissolve quite quickly. Traces of iron, manganese, magnesium and strontium evident in various stages of the experiment suggest the some dissolution may occur from the stainless steel basket containing the samples, and also from the stainless steel reservoirs of the geothermal cell.

Preliminary attempts at quantification of these minerals has been carried out using x-ray diffraction (XRD) and x-ray fluorescence (XRF) for major elements analysis, also using the Rietveld refinement for mineralogical compositions.

XRD Analysis of Samples over time

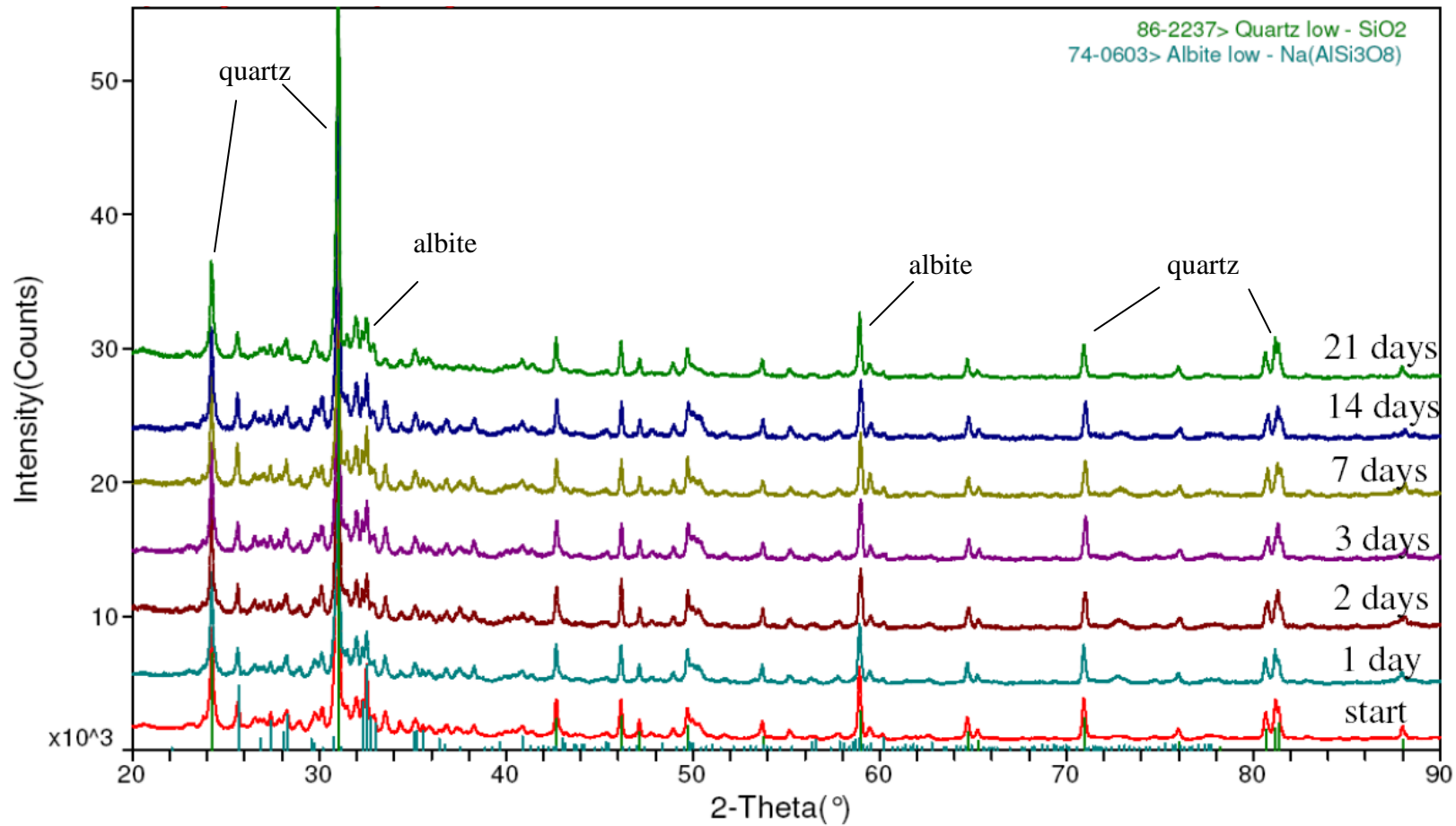


Figure 3.16: Temporal XRD patterns from geothermal-cell experiments over a 21 day period.

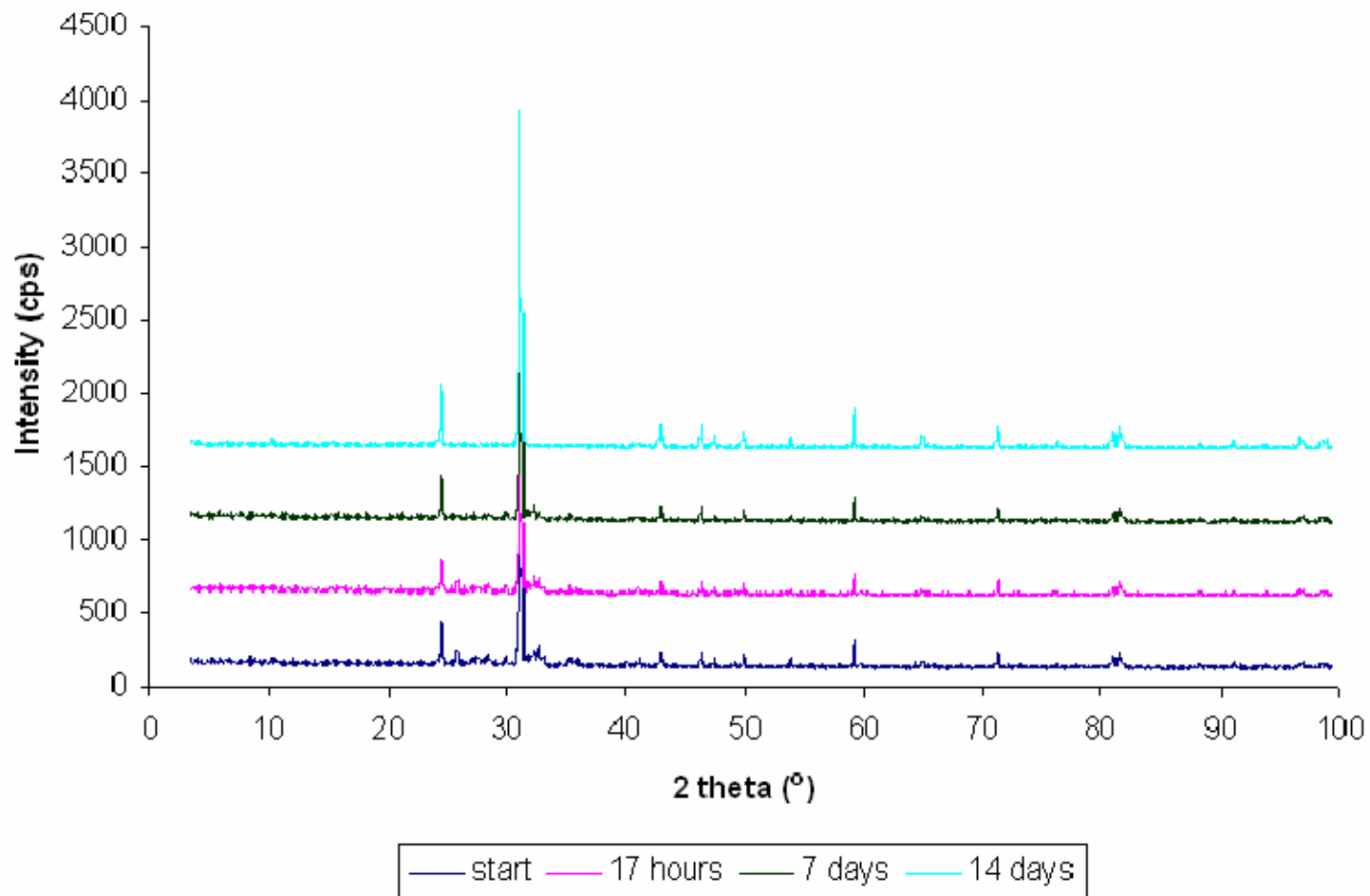


Figure 3.17: Temporal XRD patterns from ultrasonically cleaned samples over a 14 day period

Figure 3.16 provides a temporal sequence of XRD patterns for the sample over a 21 day experimental period. The following figure (figure 3.17) summarizes the XRD patterns for ultrasonically cleaned samples with fluid replacement every 24 hours. In both patterns, the dominant minerals are quartz and albite- and microcline- feldspars. Quartz concentration remains stable whilst the feldspars experiences a slight reduction. Rietveld quantitative phase analysis was attempted, but difficulties were experienced in obtaining a suitable two feldspar model for the XRD patterns which was consistent with optical microscopy and XRF analyses (Further work is currently being undertaken). T

XRF Analysis

The results of this analysis are summarised in Tables 3.3 and 3.4.

Table 3.3: Rock composition (wt%) over a 21 day period

Item % wt	Initial Material	1 day	2 days	3 days	7 days	14 days	21 days
SiO ₂	65.6	65.5	66.5	67.0	67.1	66.5	66.9
Al ₂ O ₃	9.8	9.3	9.4	9.9	11.1	10.9	10.3
Fe ₂ O ₃	4.1	4.2	4.0	3.4	3.3	3.53	3.9
MnO	0.14	0.14	0.15	0.13	0.13	0.13	0.14
MgO	0.18	0.17	0.17	0.18	0.06	0.05	0.16
CaO	1.1	1.11	1.0	1.06	1.12	1.13	1.02
Na ₂ O	2.14	1.96	1.95	2.17	2.26	2.14	2.04
K ₂ O	3.6	3.5	3.7	3.92	4.05	4.17	4.12
TiO ₂	0.11	0.10	0.09	0.10	0.08	0.08	0.09
P ₂ O ₅	0.02	0.01	0.01	0.01	0.01	0.01	0.01
SO ₃	2.4	2.03	1.90	1.8	1.56	1.65	1.83
LOI*	2.8	2.9	2.79	2.10	2.98	2.54	2.32
Total	92	91	91.6	91.9	93.8	92.8	92.8

* Lost on ignition

Table 3.4 Rock Composition (wt%) in ultrasonically cleaned rock composition over a 7 day period

Item % wt	Initial Sample	17 h later	7 days later
SiO ₂	77.3	77.5	79.0
Al ₂ O ₃	10.6	10.6	10.1
Fe ₂ O ₃	1.5	1.08	1.0
MnO	0.08	0.05	0.05
MgO	0.09	0.03	0.00
CaO	0.60	0.28	0.28
Na ₂ O	2.5	2.18	0.85
K ₂ O	4.5	4.57	4.5
TiO ₂	0.07	0.05	0.06
P ₂ O ₅	0.01	0.01	0.00
SO ₃	0.15	0.05	0.00
LOI %	2.10	2.9	1.02
Total %	99.4	99.3	96.8

Unfortunately, the amount of sample remaining by the 14th day was insufficient to conduct any analysis as roughly 80% of the sample had dissolved into the circulating fluid.

Table 3.3 summarizes the rock samples' composition. The lack of closure of the species balance is probably caused by the small sample size used in testing. The sample principally contains SiO₂, Al₂O₃, Fe₂O₃, CaO, Na₂O, K₂O and SO₃. Table 3.4 (ultrasonically cleaned samples) presents similar results. However, the levels of SiO₂, Al₂O₃, Na₂O, and K₂O are slightly higher, apparently the ultrasonic cleaning has resulted in increased dissolution of Fe, Ca and S.

The above results agree with earlier findings (Section 3.1 - Rock Analysis & Section 3.2 – Backscattered SEM Images of the Rock Samples) which suggested that the rocks are composed primarily of albite, microcline and quartz. A preliminary material balance is presented in Table 3.9. Unfortunately, not all the elements can be analysed using ICP-MS due to the constraints and interference within the equipment. Hence, the material balance is incomplete but most major elements have been quantified. Hence, the balance does provide a preliminary representation of the dissolution reaction.

Water Analysis

Figures 3.18-3.21 present data for the uncleaned samples whilst Figures 3.22-3.29 are for the ultrasonically cleaned samples

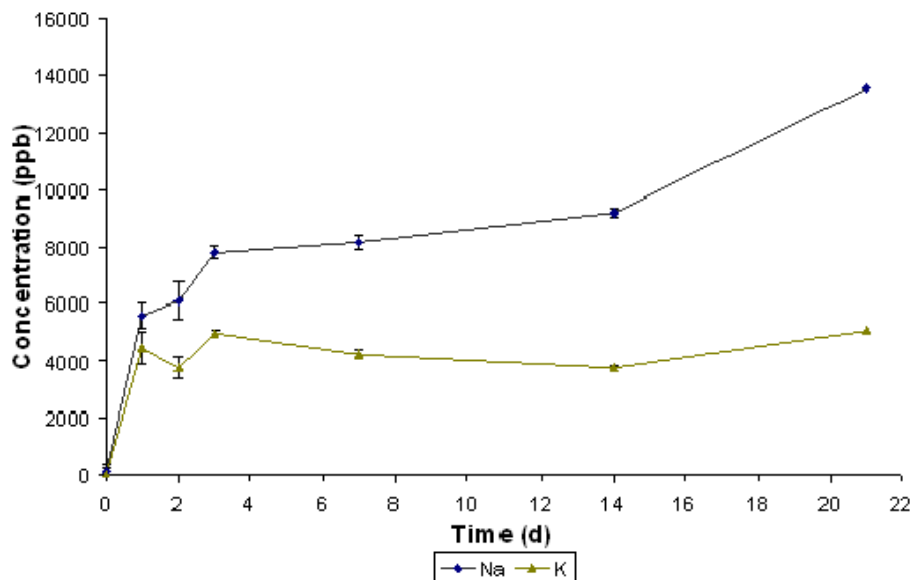


Figure 3.18 : ICP-MS results showing concentrations of Na and K as a function of time.

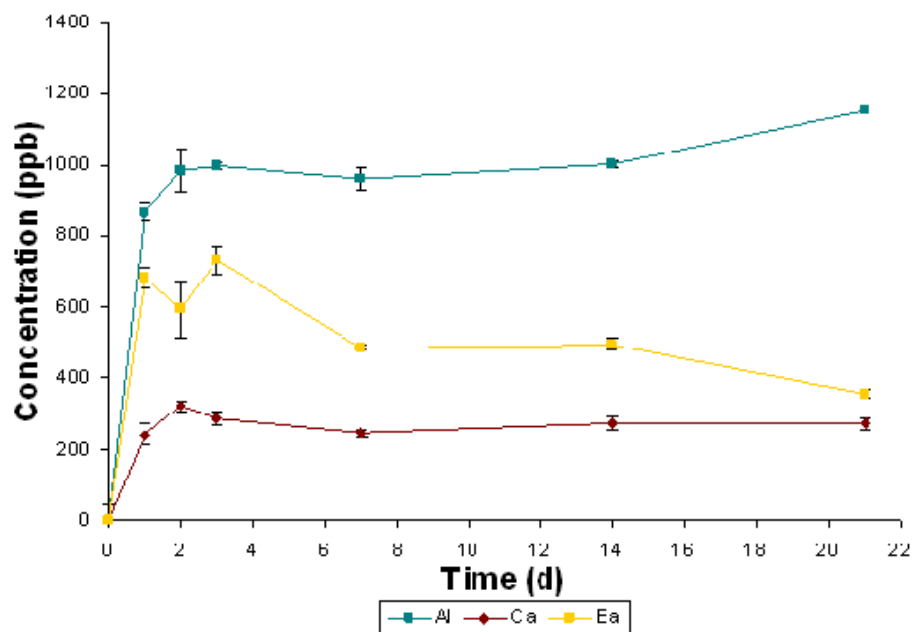


Figure 3.19: ICP-MS results showing concentrations of Al, Ca and Ba as a function of time.

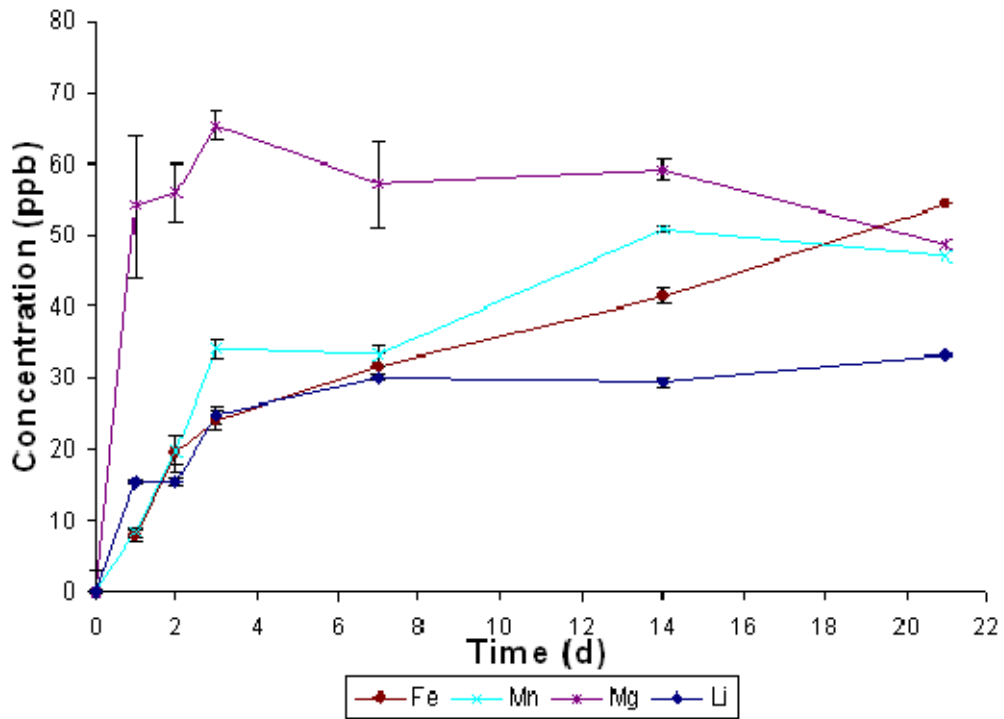


Figure 3.20: ICP-MS results showing concentrations of Fe, Mn, Mg and Li as a function of time.

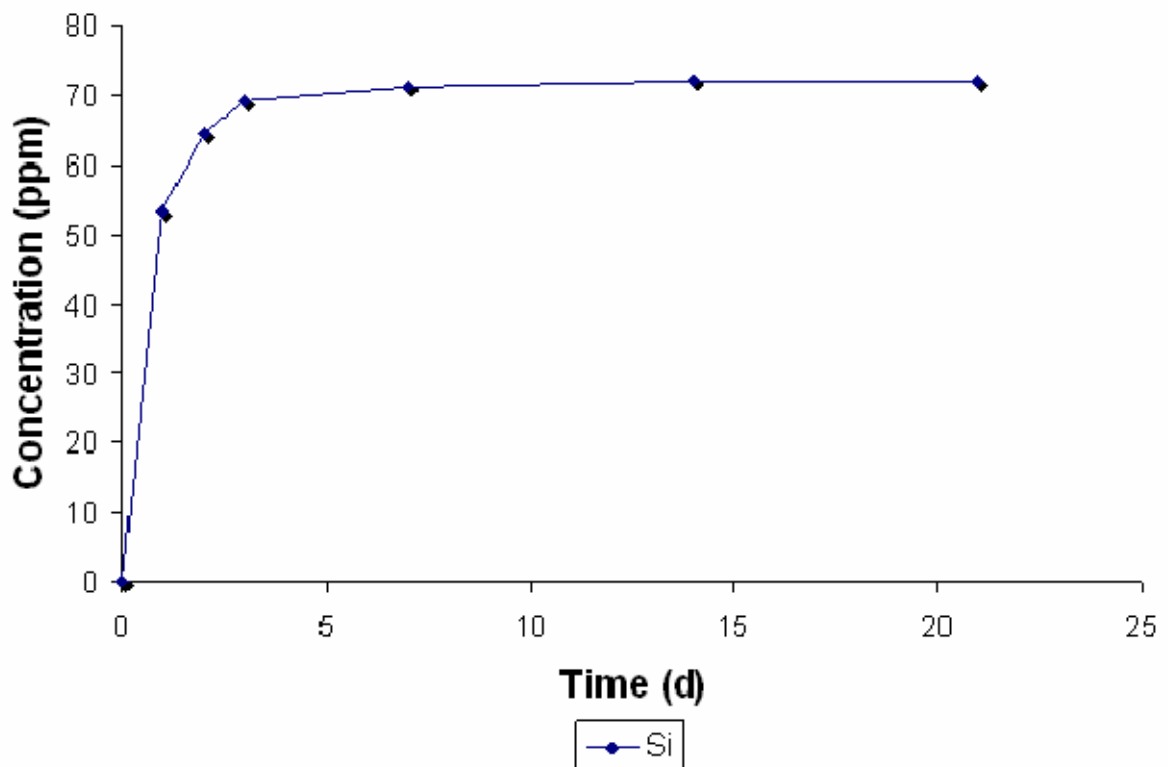


Figure 3.21: ICP-MS results showing concentration of Si as a function of time.

The initial water pH was 5.5 and this value did not change significantly for all batch experiments independent of their duration. Figures 3.18-3.21 show the concentration of elements versus time. The silica concentration was obtained using Hach spectrophotometric method whilst other elements were analysed using Solution ICP-MS.

The results confirm that dissolution occurs as a consequence of the rock water interaction. In general, significant dissolution of the minerals occurs as indicated by the rise in concentration of metal species in the liquid phase. Such rapid dissolution is probably a consequence fine particle dissolution. Such particles readily adhere to the mineral grains (Figure 3.8). As well, the replacement of the circulation fluid with pure water over a 24 hour cycle will contribute significantly to the dissolution reaction.

Increases in concentrations of elements Si, Al, Na, and K in the liquid phase suggest some dissolution of albite and microcline feldspars. Whereas, increases in the concentrations of Fe Mg and Mn in the liquid phase may result from carbonate dissolution.. Concentration of all analysed elements showed a net increase during the experiment, with the notable exception of Ca, Ba and Mg.

Water analysis with ultrasonically cleaned samples

Results from the set of experiments to observe the effects of the circulation of newly injected fresh water are shown in this section. Table 3.5 shows the concentration of elements after 17 hours of flow.

Table 3.5 Concentration of elements after 17 hours of circulation time

Elements	Concentrations (ppb)
Li	4.1
Na	8400
Al	1245
K	3125
Fe	91.5
Ba	302.1
Mn	8.9
Mg	32.3
Si	38.1

Figures 3.22 – 3.29 present the cumulative concentration of elements versus time.

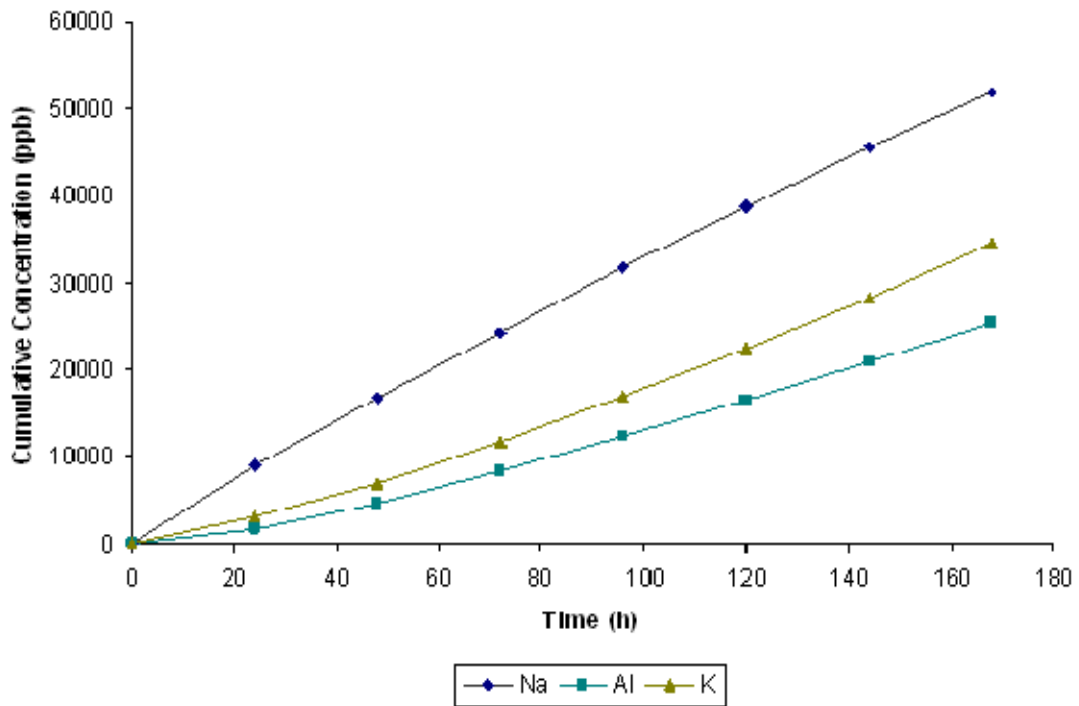


Figure 3.22: Cumulative concentrations (ICPMS) of Na, Al, and K over a 7 day period

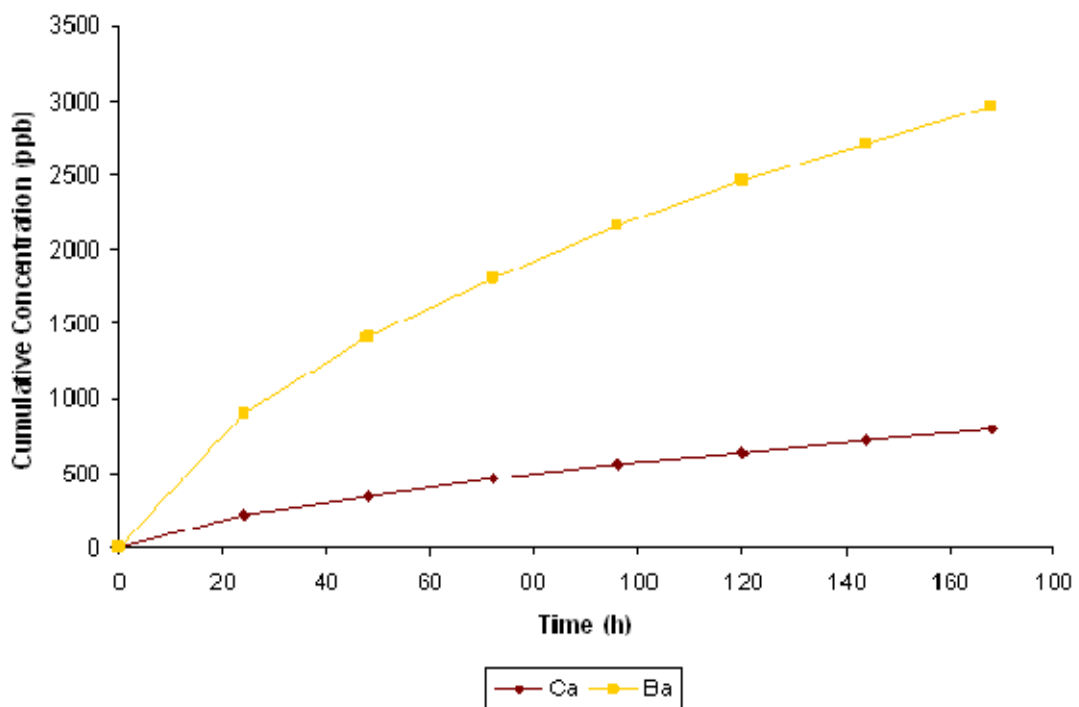


Figure 3.23: Cumulative concentrations (ICPMS) of Ca and Ba over a 7 day period

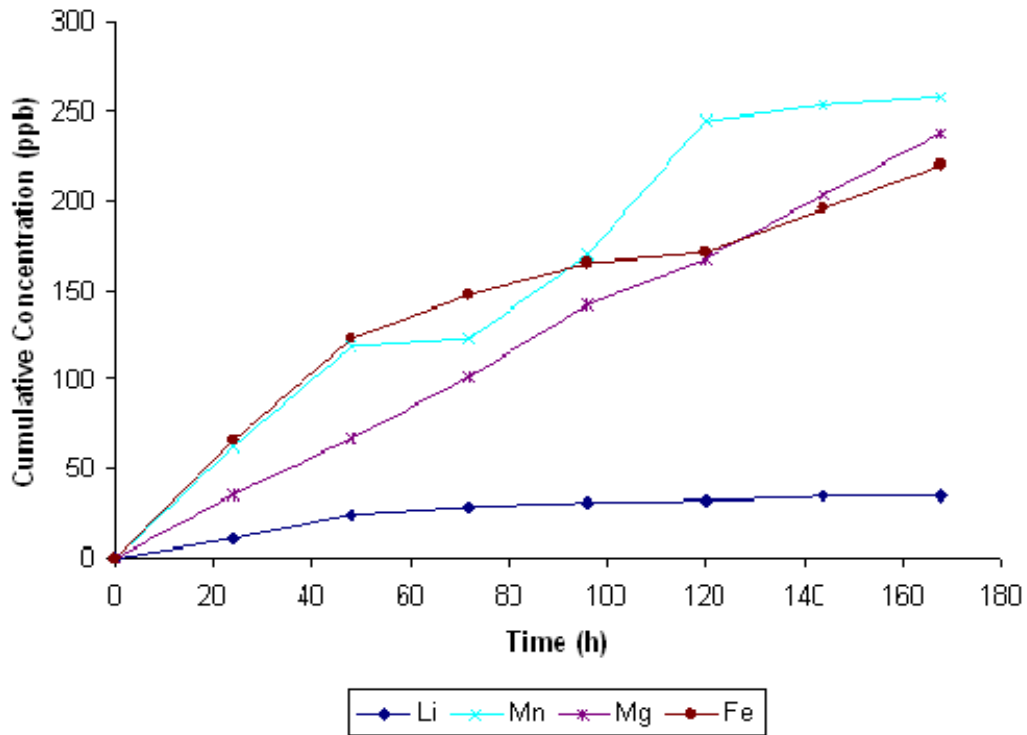


Figure 3.24: Cumulative concentrations (ICPMS) of Li, Mn, Mg, and Fe over a 7 day period

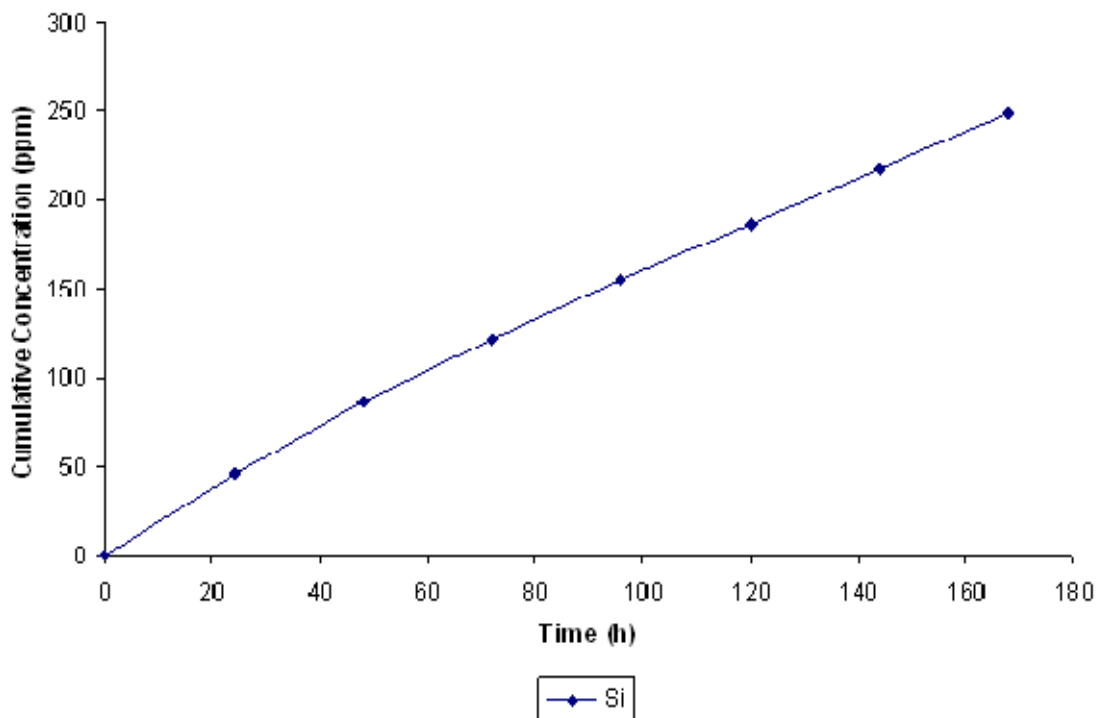


Figure 3.25: Cumulative concentrations (Hach method) of Si over a 7 day period

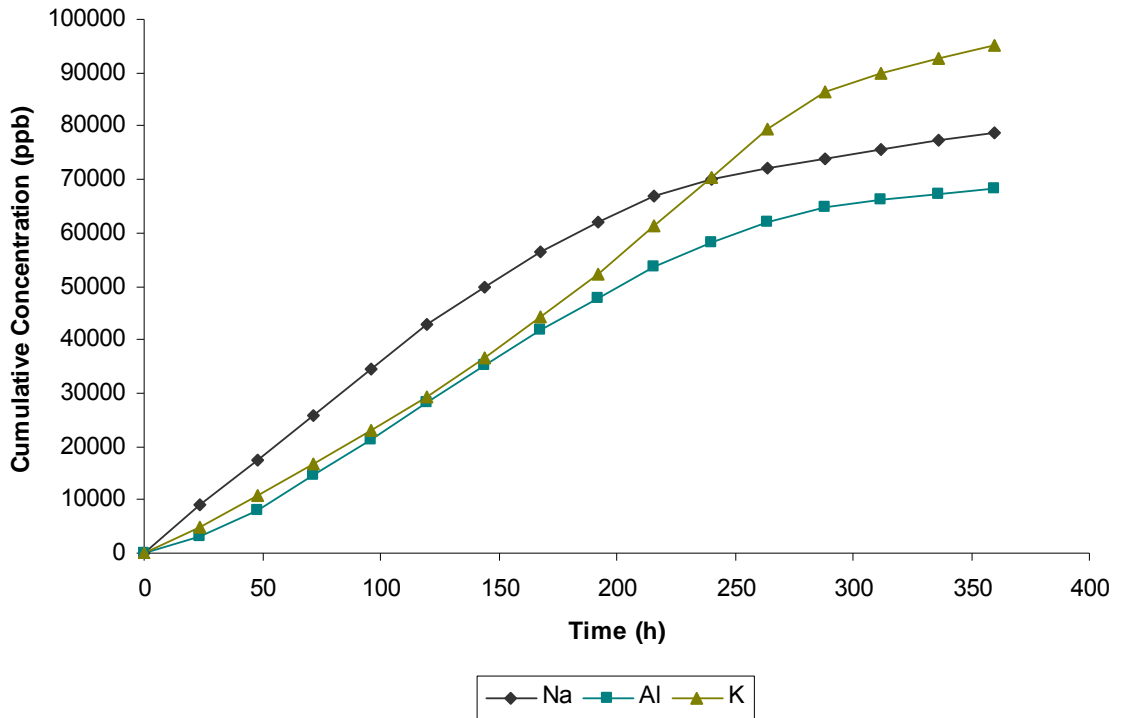


Figure 3.26: ICP-MS results showing cumulative concentrations of Na, Al, and K for 14 days

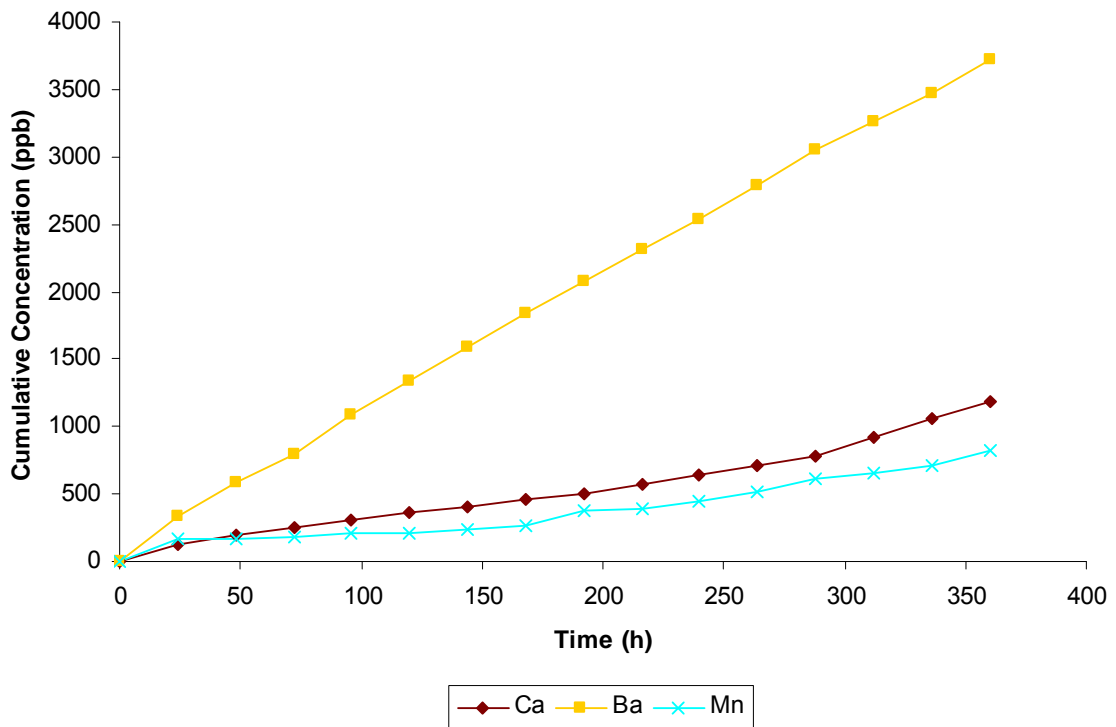


Figure 3.27: Cumulative concentrations (ICPMS) of Ca, Ba, and Mn over a 14 day period

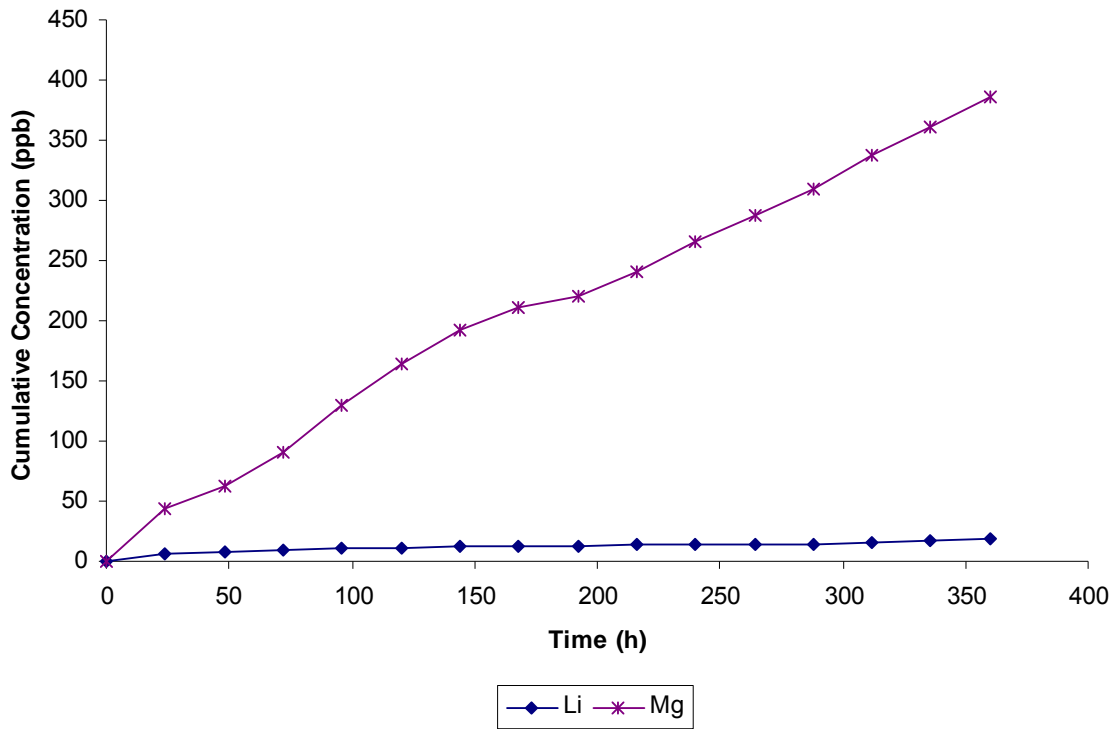


Figure 3.28: Cumulative concentrations (ICPMS) of Li and Mg over a 14 day period.

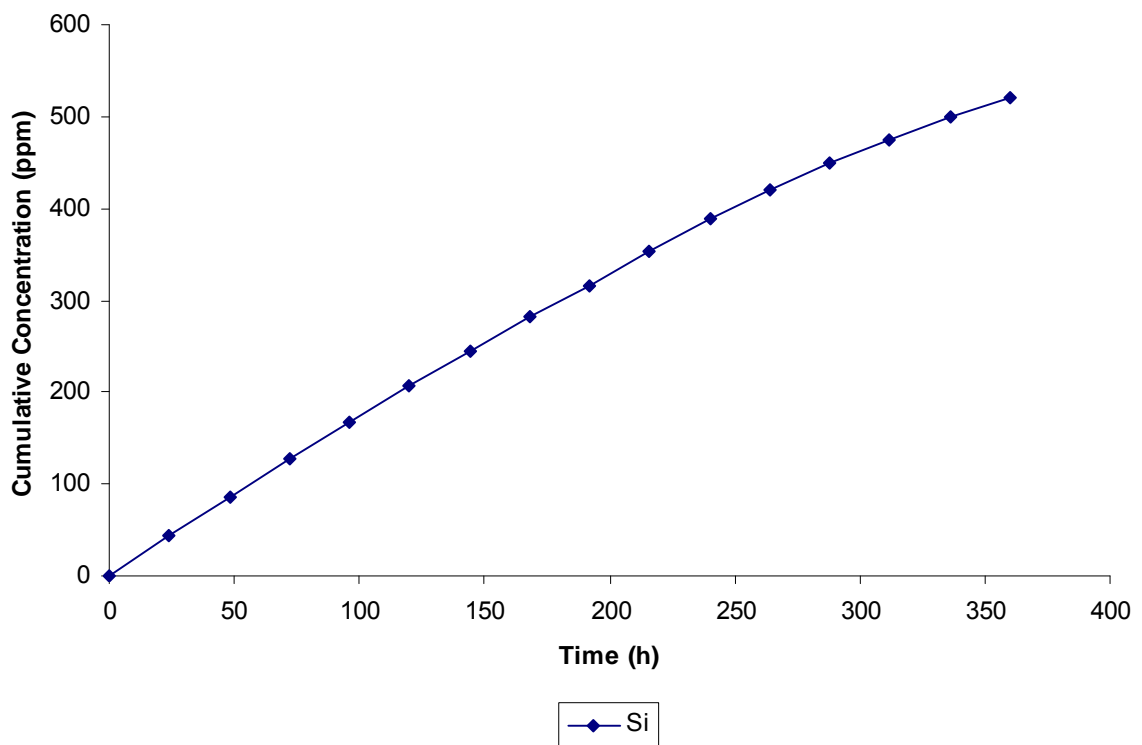


Figure 3.29: Cumulative concentrations (Hach Method) of Si over a 14 day period

As for the earlier test the initial pH of the water was 5.5 and remained constant. After every 24 hours, the circulating water removed from the flow through cell, preserved and stored. Each sample was analysed, and the concentration results were combined (added) thereby producing a cumulative concentration. As expected, greater dissolution occurs when compared to the previous set of experiments.

Mass Balances on the System

Table 3.6 Initial elemental masses of rock samples derived from XRF data (mg)

Elements (mg)	1 day	2 days	3 days	7 days	14 days	21 days	U/C* 17 hours	U/C 7 days
Si	230.88	231.37	320.01	232.26	225.52	238.52	261.82	265.36
Al	38.95	39.03	53.98	39.18	38.04	40.24	40.75	41.30
Fe	21.59	21.63	29.92	21.72	21.09	22.30	7.39	7.49
Mn	0.79	0.79	1.10	0.80	0.77	0.82	0.43	0.44
Mg	0.79	0.80	1.10	0.80	0.78	0.82	0.41	0.41
Ca	5.96	5.97	8.26	5.99	5.82	6.15	3.09	3.13
Na	11.96	11.99	16.58	12.03	11.68	12.36	13.67	13.85
K	22.46	22.51	31.13	22.59	21.94	23.20	26.76	27.12
Ti	0.71	0.71	0.98	0.71	0.69	0.73	0.42	0.43
P	0.05	0.05	0.05	0.05	0.05	0.05	0.04	0.04
S	7.37	7.39	7.41	7.41	7.20	7.61	0.44	0.45

* U/C denotes samples which were ultrasonically cleaned

Table 3.7 Final elemental masses of rock samples derived from XRF data (mg)

Elements (mg)	1 day	2 days	3 days	7 days	14 days	21 days	U/C 17 hours	U/C 7 days
Si	204.35	202.60	280.35	192.79	178.20	188.56	236.14	164.94
Al	33.00	32.53	46.93	36.18	33.01	32.83	36.39	23.78
Fe	19.51	18.34	21.37	14.17	14.17	16.33	4.93	3.16
Mn	0.74	0.73	0.93	0.59	0.58	0.63	0.27	0.17
Mg	0.67	0.66	0.98	0.23	0.17	0.57	0.11	0.00
Ca	5.32	4.60	6.80	4.89	4.64	4.38	1.32	0.90
Na	9.72	9.43	14.42	10.27	9.08	9.10	10.53	2.81
K	19.62	20.00	29.11	20.65	19.87	20.64	24.74	16.65

Ti	0.57	0.51	0.76	0.42	0.41	0.48	0.26	0.25
P	0.04	0.03	0.05	0.02	0.02	0.03	0.02	0.00
S	5.42	4.97	6.42	3.83	3.79	4.42	0.14	0.01

Table 3.8 Composition of water samples from experiments

Elements (mg)	1 day	2 days	3 days	7 days	14 days	21 days	U/C 17 hours	U/C 7 days
Si	13.587	16.436	17.592	18.116	18.355	18.355	9.702	63.479
Al	0.221	0.251	0.255	0.245	0.256	0.294	0.318	6.470
Fe	0.002	0.005	0.006	0.008	0.011	0.014	0.023	0.056
Mn	0.002	0.005	0.009	0.008	0.013	0.012	0.002	0.066
Mg	0.014	0.014	0.017	0.015	0.015	0.012	0.013	0.060
Ca	0.062	0.082	0.073	0.063	0.070	0.069	0.058	0.203
Na	1.427	1.559	1.990	2.080	2.350	3.461	2.143	13.215
K	1.137	0.958	1.269	1.081	0.952	1.294	0.797	8.786

Material balance equation:

$$m_i = m_o + d + \text{error (loss)}$$

where:

m_i = mass of element before experiment, mg

m_o = mass of element after experiment, mg

d = mass of dissolved element, mg

Sample calculation for silica, taken from 1 day data:

$$m_i = m_o + d + \text{error (loss)}$$

$$230.88 = 204.35 + 13.59 + \text{error (loss)}$$

$$\text{Error (loss)} = 12.95 \text{ mg}$$

Table 3.9 Calculated loss or error from the material balance

Loss	1 day	2 days	3 days	7 days	14 days	21 days	U/C 17 hours	U/C 7 days
Si	12.95	12.33	22.08	21.36	28.96	31.60	15.98	36.94
Al	5.73	6.25	6.80	2.76	4.77	7.11	4.04	11.04
Fe	2.08	3.29	8.54	7.54	6.91	5.96	2.44	4.28
Mn	0.05	0.06	0.16	0.19	0.18	0.18	0.16	0.21
Mg	0.11	0.13	0.11	0.55	0.59	0.24	0.28	0.35
Ca	0.58	1.29	1.38	1.04	1.11	1.71	1.71	2.03
Na	0.81	1.00	0.17	-0.32	0.25	-0.21	1.00	-2.17
K	1.70	1.55	0.75	0.86	1.11	1.27	1.22	1.69

4. Supporting Activities

Water and Rock samples were collected at the Habanero site on 31 July 2008 by A/Prof. Brian O'Neill, Dr Yung Ngothai and Mr Gideon Kuncoro (PhD student).

Mr Gideon Kuncoro and Dr Yung Ngothai attended the AGEC 2008, Melbourne, 19-22 August 2008.

Dr Yung Ngothai attended the Geothermal Research Council Annual Meeting in Reno, Nevada, 4-7 October 2009.

A technical seminar based on this project was presented by Dr Yung Ngothai to 15 researchers at the Institute for Geo-Resources and Environment, National Institute of Advanced Industrial Science and Technology (Japan).

A PhD research proposal was presented by Gideon Kuncoro (March 2009) to 40 attendees including 3 staff from PIRSA at the School of Chemical Engineering.

A/Prof. Brian O'Neill will be presenting the outcome of the work of this project at the AGEC 2009, Brisbane, 10-13 November 2009.

Appendix:

Paper to be presented at AGECE 2009, 10-13 November.